ACR No. L4L21

NATIONAL ADVISORY COMMITTEE FOR AERONAUTICS

WARTIME REPORT

ORIGINALLY ISSUED

January 1945 as
Advance Confidential Report L4L21

SUMMARY OF DATA RELATING TO THE EFFECTS OF WING MACHINE-GUN AND CANNON INSTALLATIONS ON THE AERODYNAMIC CHARACTERISTICS OF AIRPLANES

By John H. Quinn, Jr.

Langley Memorial Aeronautical Laboratory
Langley Field, Va.

WASHINGTON

NATIONAL ADVISORY COMMITTEE FOR AERONAUTICS

ADVANCE CONFIDENTIAL REPORT

SUMMARY OF DATA RELATING TO THE EFFECTS OF WING MACHINE-GUN AND CANNON INSTALLATIONS ON THE AERODYNAMIC CHARACTERISTICS OF AIRPLANES

By John H. Quinn, Jr.

SUMMARY

Data obtained from tests of models and airplanes relating to the effects of various wing armament installations have been collected and analyzed. Three types of gun installation were considered; namely, gun ports (submerged machine guns), protruding machine guns, and cannon. Data have been presented as drag-coefficient increments of one gun based on an area equal to the square of the local wing chord and as incremental lifts for the complete installation based on airplane (or model) wing area.

The analysis of these data revealed that a well-designed gun port should have little or no effect on either the drag or maximum lift of an airplane. A well-designed gun opening in the leading edge of a wing should not exceed one-tenth of the wing thickness in height, should have provision for air flow and be fitted with a suitable exit vent, and should be located on or a few percent of the chord below the chord line. Gun ports that did not fall in this category were found to cause drag-coefficient increments up to 0.0018 and to decrease maximum lift coefficient by as much as 0.12. Gun openings at least up to 25 percent of the local wing thickness in height may yield small drag increments, however, provided a faired nose-air-intake shape is used.

The smallest drag-coefficient increments for protruding-machine-gun installations were obtained with machine guns that protruded approximately 4 percent of the wing chord ahead of the leading edge of the wing, were located on or near the chord line, and were faired smoothly into the wing contour. Unfaired guns with greater extensions caused drag-coefficient increments

up to 0.0010, and guns mounted below the wing caused increments of 0.0038. Gun extensions of at least 0.25 chord, however, were found to have less adverse effect on maximum lift than shorter extensions.

The drag-coefficient increments caused by cannon installations on the wing were decreased approximately 0.0003 or 0.0004 by fairing the cannon into the wing and providing air flow. Cannon located below the chord line caused increments of 0.0038, or nearly four times the increment of an unfaired cannon mounted on the wing. Faired cannon located on the wing generally had little or no effect on maximum lift. Unfaired cannon located on the wing and faired cannon located below the wing were found to decrease maximum lift coefficients by as much as 0.09.

INTRODUCTION

A number of investigations conducted by the National Advisory Committee for Aeronautics during the past few years have dealt in part with the effects of wing-armament installations on the aerodynamic characteristics of airplanes. The purpose of the present report is to group these data in some logical fashion to facilitate their analysis and to establish, wherever possible, trends for correct design.

The armament installations considered fall logically into three groups: gun ports (submerged machine guns), protruding machine guns, and cannon. An analysis of the data revealed some definite trends that should be of considerable aid in the design of improved wing-armament installations. A discussion of the test results and of the various factors affecting the aerodynamic design of wing-armament installations is given in the following sections.

SYMBOLS

C_D airplane drag coefficient

C_L airplane lift coefficient

c_l	section lift coefficient
c_{d_o}	section profile-drag coefficient
ΔC_{D_c}	incremental wing-gun drag coefficient based on local wing chord squared $\left[\frac{S}{nc^2}\left(C_{D_{model + guns}} - C_{D_{model}}\right)\right]$
n	number of guns
c	local wing chord at center of gun installation
S	wing area
t	maximum wing thickness
h	height of gun-port opening
e	extension of gun or cannon ahead of wing
A_i	gun-port inlet area
A_e	exit area of gun duct
$\pm\Delta C_{L_{max}}$	increment (+) or decrement (-) in maximum lift coefficient
R	Reynolds number
δ_f	angular deflection of flap
V_o	free-stream velocity
V_i	gun-port inlet velocity

TESTS

The data presented herein were obtained from two-dimensional wind-tunnel tests of rectangular wings, three-dimensional wind-tunnel tests of scale models, and full-scale wind-tunnel and flight tests of airplanes. For the two-dimensional tests, the drag was determined by the wake-survey method and lift was determined by

integrating the pressure along the floor and ceiling of the tunnel test section (reference 1). In all the other tunnels, lift, drag, and moment were obtained from balance measurements. Standard methods of speed determination were used in obtaining the flight-test data.

PRESENTATION OF DATA

The lift- and drag-coefficient increments, together with the important dimensions, are presented in table I for the submerged machine-gun installations, in table II for the protruding machine-gun installations, and in table III for the wing-cannon installations. Drag-coefficient increments, detailed sketches, and photographs of the various installations are presented in figures 1 to 43.

The tables alone should not be used to compare the various installations but should be supplemented by comparing the plots of drag-coefficient increment against lift coefficient. Because of experimental inaccuracies and the variation with lift coefficient, the drag increments at any one lift coefficient may not give a true indication of the relative merits of different installations.

Lift effects are shown for only three-dimensional models; the incremental coefficient is for the complete armament installation and is based on total wing area. In order to facilitate the analysis and use of the drag data, however, the increments have been presented in terms of the coefficient ΔC_{D_c}.

PRECISION OF MEASUREMENTS

In order to facilitate comparison of the data obtained in the different tunnels, probable errors in drag-coefficient increment have been estimated and are presented in tables I to III. The experimental accuracy was assumed to be ±1 percent of the total measured drag for all data not obtained by the wake-survey method. This accuracy is thought to approximate the limits within which a point may be checked, as determined from past experience.

In determining the error involved in the wake-survey data, a slightly different procedure was followed. In addition to a probable error of 1 percent in the drag-coefficient increment, there was the possibility that the spanwise drag curve might not taper off to the correct plain-wing drag at either end. For each of the tests made by the wake-survey method, therefore, the error given in tables I to III was obtained from the expression:

$$\text{Error} = 0.01\,\Delta C_D + \text{Estimated error due to curves not returning to correct base lines}$$

The values of the probable errors in the drag-coefficient increments of armament installations as measured on a wing model and on an airplane or model of the airplane differ considerably. This difference occurs because the drag of a gun installation on a wing model often is of the same order of magnitude as the drag of the model, whereas the drag of the armament installation on a complete airplane is but a very small part of the airplane drag.

DISCUSSION

The discussion of the data presented is divided into three sections: gun-port, protruding machine-gun, and cannon installations. Under each of these headings, the effect of several significant parameters on the lift and drag characteristics of the model upon which the guns were mounted is discussed. Although the greater part of the discussion deals with the effect of wing guns on the drag of the airplane, maximum lift effects are presented wherever available. The available tests showed that the effects of wing-armament installations on the pitching-moment characteristics of an airplane were negligible. Pitching-moment data, therefore, are not presented.

In several cases, the results obtained with gun installations on airplanes do not agree with the results obtained with gun installations on models. The effect of an actual gun installation depends to a large extent upon the surface condition of the wing upon which it is mounted, because rough wing surfaces or poor wing construction may partly mask the adverse effects of a

relatively poor gun installation. In order to find the true effect of an armament installation on a particular airplane, therefore, full-scale data should be used. Data from model tests are used in the determination of the separate effects of the various factors that enter into the aerodynamic design of a wing-armament installation.

Gun Ports (Submerged Machine Guns)

The effects of a well-designed gun port on the aerodynamic characteristics of a smooth wing are small. The important factors to be considered in the design of such a gun port are discussed in the following order: the air flow through the gun port, the height of the port with respect to the wing thickness, and the position of the gun port with respect to the wing chord line.

The effect of air flow on the drag-coefficient increment of a gun port was investigated by tests with and without air flow on a model of the wing of the XP-47B airplane (table I, fig. 1). At a lift coefficient of 0.2 without air flow the gun port caused a drag-coefficient increment of 0.0005, whereas the same port with air flow caused an increment of only 0.0001. From this result it appears advantageous to provide a suitable exit vent for the gun port and to permit the air to flow around the gun and to exhaust at some point on the wing. In this test the air was vented to the upper part of the aileron slot. In practice, air usually flows through the gun port, although a suitable exit vent is rarely provided. In most cases, the air that enters the gun port leaks out into the air stream through a wing joint or through the fuselage. The advantage of having air flowing through the gun port is thus partly realized, but the gain is often more than offset by the power required to overcome the loss resulting from leakage, which causes an external disturbance. Inasmuch as some air almost always flows through the port of an actual installation, the greater part of the discussion will deal with the analysis of the aerodynamic effects of other parameters with air flowing.

The wing of the XP-63 airplane (table I, figs. 2 and 3) and a model of the modified XP-41 airplane

(table I, figs. 4 and 5) were tested to find the effect of gun-port height on the drag-coefficient increment caused by a gun port. (See reference 2.) Increasing the gun-port height is shown to increase the drag increment. The drag increment for the gun port on a model of the XF4U-1 airplane, which has a large inlet height (table I, figs. 6 and 7) was about the same as the increment for the larger gun port on the model of the modified XP-41 airplane. From inspection of these data and of those for the XP-47B wing section, gun ports having a height up to approximately 10 percent of the wing thickness (0.10t) appear to cause little or no increase in the wing drag. Tests of the F4U-1 (table I, figs. 8 and 9) and XF2A-2 (table I, figs. 10 and 11) airplanes in the Langley full-scale tunnel show lower drags than would be predicted from model tests. Inasmuch as the wings of these airplanes were unusually rough, it might be expected that the adverse effects of large gun-port heights are partly masked in these cases.

A low-drag gun port with three types of front opening was developed (table I, figs. 12 and 13, and reference 3) to obtain a gun port having a height that was large with respect to the wing thickness and yet having low drag. The gun openings, which are 25 percent of the thickness of the bulged portion of the wing in height, owe their low-drag properties to a faired nose-air-intake shape at the entrance. These inlets were designed by use of the findings of the tests reported in reference 4. If it is necessary to have an opening that is large with respect to the wing thickness, a similar faired nose-opening shape should be used. Large openings may possibly be avoided by moving the breech of the gun for aiming rather than the muzzle. Small openings and consequently low drag increments would then be possible.

In order to determine the effect on drag of the position of the gun ports with respect to the chord line of the wing, a comparison was made of the drag-coefficient increments for the gun ports 0.5 percent chord (0.005c) and 2.6 percent chord (0.026c) above the chord line of the wing of the XF2A-2 airplane (table I, figs. 10 and 11, and reference 5). The gun-port position nearer the chord line was found to result in the smaller increment. Similarly, it is seen from table I and figure 3(a) that a gun port 0.018c high

by 0.033c wide centered on the chord line of a model of the wing of the XP-63 airplane caused a negligible increase in drag. Comparison of the spanwise drag surveys for similar gun ports on and slightly below the chord line (fig. 3), however, showsno important difference resulting from positions on the chord line and below the chord line. Because of the limited travel of the survey apparatus, it was difficult to obtain a complete spanwise drag survey for these gun ports, but reasonable estimates of the extent of the curves and the area under them (proportional to the drag increment) may be made. Gun ports 0.012c by 0.026c and 0.015c by 0.027c centered 0.014c below the chord line, both of which are smaller in height and width than the 0.018c by 0.033c gun port on the chord line, caused somewhat larger drag increments than the gun port on the chord line. The 0.033c by 0.033c gun port centered below the chord line, however, probably has a slightly smaller drag than the 0.021c by 0.033c gun port on the chord line. These results indicate that gun ports centered on or slightly below the chord line caused smaller drag increments than gun ports centered above the chord line. A reasonable explanation for this conclusion may be obtained from consideration of the stream lines about the wing at the cruising lift coefficient. If the cruising lift coefficient is equal to or greater than the design lift coefficient of the wing, the stagnation point is at or slightly below the chord line. Gun ports centered above the chord line, in a high-velocity region, thus have more adverse effect than gun ports located in the low-velocity region in the neighborhood of the stagnation point.

The drag-coefficient increments for gun ports on a model of the wing of the XA-41 airplane, where no air flow was provided (table I, figs. 14 to 16), showed that the gun ports on or near the chord line caused larger drag increments than those above or below the chord line, and these drag increments without air flow in nearly every case were much larger than any measured with air flow. One such gun port, $16\frac{1}{2}$ percent of the wing thickness in height and centered slightly above the chord line, caused a drag-coefficient increment of 0.0018. Without air flow, the gun ports on or near the chord line, depending upon their size, probably

spoil flow on both surfaces, whereas gun ports above or below the chord line spoil flow on only one surface. The gun ports above the chord line caused larger drag increments than gun ports centered below the chord line even without air flow.

Three gun-port configurations were tested on the P-51B airplane in the Langley full-scale tunnel (table I, figs. 17 and 18). The gun port was tested (1) in the service condition (gun port open), (2) covered with tape that was torn to simulate the conditon after firing, and (3) covered with metal plates having holes just large enough to allow the passage of a bullet. The results of these tests are given in table I and figure 18. The taped gun ports gave slightly lower drag increments than the service gun ports. The cover plates having small holes resulted in the best arrangement tested on this airplane.

An examination of the effect of the various gun ports on the maximum lift coefficient (table I) indicates that few of the installations had serious adverse effect. The large loss in maximum lift coefficient of 0.12 on the P-51B airplane probably occurred because the gun port was 26 percent of the wing thickness in height.

Protruding Machine Guns

Because of space limitation or other considerations, it is often necessary to install machine guns that protrude ahead of the leading edge of the wing. The most important variables affecting the design of a protruding machine-gun installation from aerodynamic considerations are the position of the gun with respect to the chord line and the extension of the gun barrel ahead of the leading edge of the wing.

Several gun extensions and two positions with respect to the wing chord line were tested on the XF2A-2 airplane in the Langley full-scale tunnel (table II, figs. 19 and 20). An extension of 0.028c caused a lower drag-coefficient increment than a 0.139c extension, but the drag of the 0.139c extension was essentially the same as that of the 0.254c extension. The 0.139c extension was tested 0.005c and 0.026c above the chord line. The position nearer the chord line

yielded the lower drag increments. Protruding machine-gun installations were also tested on a model of the modified XP-41 airplane and on the F6F-3 airplane (table II, figs. 21 to 23). The 0.100c extension on the modified XP-41 airplane caused about the same drag as the 0.139c extension 0.005c above the chord line of the wing of the XF2A-2 airplane. The lowest drag-coefficient increment for protruding machine guns ($\Delta C_{D_c} = 0.0001$) was obtained with the 4-percent-chord extension mounted 0.02c above the chord line of the wing of the F6F-3 airplane. For these tests, the guns were provided with a well-designed smooth fairing. The 0.19c gun extension on the XP-63 wing model (table II, figs. 24 and 25) caused the highest drag-coefficient increment ($\Delta C_{D_c} = 0.0010$) of any protruding gun mounted on or near the chord line. The large drag increment of this installation is due to the laminar flow that was spoiled on the low-drag wing. From the foregoing results, it appears that short well-faired gun extensions and mounting positions on or near the chord line will have the lowest drag.

Underslung machine guns were tested on a model of the wing of the XP-63 airplane, on the P-63A airplane, and on a model of the XA-26 airplane. Sketches and drag data for these arrangements are presented in table II and figures 24 to 27. A comparison of the drag of the underslung arrangements and the drag of the arrangements having guns fixed at or near the chord line (table II) shows that the drag-coefficient increments caused by the underslung guns, often as much as 0.0038, are excessive. At a lift coefficient of 0.2, the underslung arrangement on the XP-63 wing model caused an increment approximately 60 percent greater than the gun mounted on the chord line. (See fig. 25.) The installation on the P-63A airplane, which represents the manufacturer's best attempt to reproduce the model installation, caused a drag increment approximately twice that of the model installation. Sealing the ejection slots and the annular space between the gun barrel and fairing on the airplane reduced the drag increment of this installation slightly. The poor agreement between the installation and the model installation tested in the Langley two-dimensional low-turbulence pressure tunnel is probably due to leakage around the barrel through the holes in the cooling jacket on the actual installation.

Some observations concerning the effect of gun extensions on maximum lift may be made by comparing the decrements measured on the XF2A-2 airplane in the Langley full-scale tunnel (table II). The 0.028c extensions mounted 0.026c above the chord line decreased the maximum lift coefficient 0.14, whereas the 0.139c extensions mounted 0.005c above the chord line caused a decrease of 0.13. The 0.254c extension, however, mounted 0.005c above the chord line decreased the maximum lift coefficient by 0.09. It appears that gun extensions of at least 0.25c are less detrimental to maximum lift than shorter extensions - probably because the separation at the tip of the short extension passes close to the upper surface of the wing and spoils the flow, whereas this separation for the long guns passes farther above the wing and has less detrimental effect.

A number of wing-gun fairings were tested in flight on the F4F-3 airplane to improve the maximum lift and stalling characteristics. (See reference 6.) Photographs of the various fairings are presented in figure 28. The addition of unfaired guns to the otherwise clean airplane caused a considerable increase in stalling speed. Tests of a number of fairings indicated that a faired sealed opening for the submerged gun and a sealed fairing on the protruding gun resulted in practically no change in stalling speed from that of the plain wing and also aided in correcting the poor stalling characteristics of the airplane. Unsealing these fairings, however, caused a loss in maximum lift coefficient of 0.26. The pertinent data for these arrangements are given in table II.

Wing-Cannon Installations

Wing-cannon installations may be best compared on the basis of the mounting position with respect to the chord line, the type of cannon fairing, and the provision for air flow.

Two underslung and one partly submerged cannon installations were tested on the XF2A-2 airplane in the Langley full-scale tunnel (table III, figs. 29 and 30). At a lift coefficient of 0.2 the best underslung arrangement caused a drag-coefficient increment ($\Delta C_{D_c} = 0.0038$) 170 percent greater than the partly

submerged installation. This result again shows that the drags of underslung arrangements are excessive.

Cannon installations on a conventional airfoil section and several low-drag sections were tested in the Langley two-dimensional low-turbulence pressure tunnel (table III, figs. 31 and 32). As might be expected, the increment in drag coefficient was greater on the low-drag sections than on the conventional section since more laminar flow was spoiled on the low-drag sections (fig. 32(a)). Tests with two different cannon extensions and with a rough spot on the leading edge of the NACA 66(215)-216 airfoil section yielded approximately equal drag increments (fig. 32(b)). The rough spot, which was made up of carborundum grains having an average diameter of 0.01 inch attached to the airfoil with shellac, covered the same area as the cannon having the 0.16c extension. The results indicate that when a considerable amount of leading-edge area is covered by the armament installation, the amount of flow spoiled by the interference at the juncture of the cannon and wing is more important than the extension ahead of the wing. At higher lift coefficients the drag increments of the cannon exceeded that of the rough spot. Separation of the flow from the protruding cannon and the increased frontal area of the cannon are responsible for this increase in drag.

All tests of models of the XF14C-2, XF6F, and XF4U-1 airplanes in the Langley 19-foot pressure tunnel (table III, figs. 33 to 36) showed that the drag-coefficient increments caused by the wing-cannon installation may be decreased 0.0003 or 0.0004 by providing fairings similar to the ones that gave the least drag when installed on these models. The best faired cannon for these three tests caused approximately equal drag-coefficient increments regardless of the extension, position on the wing, or the airfoil section upon which they were mounted. (See fig. 36.)

Several fairings and various amounts of air flow were tested in conjunction with wing cannon on a model of the wing of the XA-41 airplane in the Ames 7- by 10-foot tunnel (table III, figs. 37 and 38). Neither the surface to which the air was discharged nor the amount of air flow had any effect upon the drag-coefficient increment, at least at inlet-velocity ratios above 0.26. At a lift coefficient of 0.2, the

drag increment of the cannon with short fairings was decreased 50 percent by providing air flow through the model. This was the lowest drag of any arrangement tested on this wing.

The faired cannon on the P-51B airplane (table III, figs. 39 and 40) caused a higher drag increment than the unfaired installations on the F4U-1 and F6F-3 airplanes (table III, figs. 41 to 43). The adverse effects of the unfaired cannon are probably partly masked by the unusually rough wings on the latter two airplanes.

Table III indicates that the unfaired cannon installation caused more adverse effect on the maximum lift coefficient than the faired cannon. As a general rule, the loss in maximum lift was greater with flaps extended than retracted. The wide fairing on the underslung cannon on the XF2A-2 airplane (fig. 29) decreased the maximum lift 0.09 (table III) as compared to a decrease of 0.04 for the narrow fairing on the underslung installation and for the partly submerged installation. A suitably faired underslung cannon installation, therefore, need not result in an appreciably greater loss in maximum lift coefficient than a partly submerged installation.

CONCLUDING REMARKS

From the analysis of the effects of wing-armament installations on the lift and drag characteristics of airplanes, the following general statements appear to be justified:

In order to decrease the drag-coefficient increments, air flow should be provided through gun ports. A suitable exit vent should also be provided to minimize the leakage losses. The drag of a gun port increases as its height increases, but a gun port with a height no greater than approximately one-tenth of the wing thickness should cause little or no additional drag. In order to obtain the smallest drag increase, gun ports should be located on or slightly below the chord line of the wing. Gun ports that satisfy the preceding conditions should have little or no effect on either drag or maximum lift. A gun port $16\frac{1}{2}$ percent of the

wing thickness in height, centered slightly above the chord line, and without air flow, caused a drag-coefficient increment of 0.0018, whereas another gun port 26 percent of the wing thickness in height decreased the maximum lift coefficient by 0.12. It is possible to use a gun opening larger than 10 percent of the wing thickness with a minimum of drag increase, however, provided a faired nose-air-intake shape is used.

Short, faired gun extensions located on or near the chord line caused the lowest drag-coefficient increments of protruding machine-gun installations. A faired gun extending 4 percent chord ahead of the leading edge of the wing and located 0.02 chord above the chord line caused a drag-coefficient increment of only 0.0001, whereas an unfaired gun centered on the chord line with a 19-percent-chord extension caused an increment of 0.0010. The drag increments of guns mounted below the wing were excessive in every case; for example, one such installation caused an increment of 0.0038.

The drag-coefficient increments caused by cannon installations on the wing were decreased 0.0003 or 0.0004 by fairing the cannon into the wing. Cannon mounted below the wing caused increments of 0.0038 or nearly four times the increment of an unfaired installation mounted on the wing. Faired cannon located on the wing generally had little or no adverse effect on maximum lift, but unfaired cannon located on the wing and faired cannon located below the wing were found to decrease maximum lift coefficients by as much as 0.09.

Langley Memorial Aeronautical Laboratory
National Advisory Committee for Aeronautics
Langley Field, Va.

REFERENCES

1. Jacobs, Eastman N., Abbott, Ira H., and Davidson, Milton: Preliminary Low-Drag-Airfoil and Flap Data from Tests at Large Reynolds Numbers and Low Turbulence. NACA ACR, March 1942.

2. Muse, Thomas C.: The Effect of Various Wing-Gun Installations on the Aerodynamic Characteristics of an Airplane Model Equipped with an NACA Low-Drag Wing. NACA ACR, July 1941.

3. Horton, Elmer A., and Woolard, Henry W.: Investigation of a Low-Drag Gun Port in the NACA Two-Dimensional Low-Turbulence Tunnel. NACA CB, Sept. 1942.

4. von Doenhoff, Albert E., and Horton, Elmer A.: Preliminary Investigation in the NACA Low-Turbulence Tunnel of Low-Drag-Airfoil Sections Suitable for Admitting Air at the Leading Edge. NACA ACR, July 1942.

5. Czarnecki, K. R., and Guryansky, Eugene R.: Tests of Wing Machine-Gun and Cannon Installations in the NACA Full-Scale Wind Tunnel. NACA ACR, Aug. 1941.

6. Nissen, J. M., and White, M. D.: Flight Investigation of Wing-Gun Fairings on a Fighter Type Airplane. NACA ACR, Oct. 1941.

TABLE I.- GUN-PORT INSTALLATIONS

Gun-port installation	Figure	Configuration	Source of data (a)	Reynolds number	Airfoil section	Wing chord (in.)	Gun-port height (percent t)	Entrance-area ratio, A_i/tc	Exit-area ratio, A_e/A_i	Gun-port position relative to chord line	Results: ΔC_{D_c} at $C_L = 0.2$ (b)	Results: $\Delta C_{L_{max}}$ (c)
	1	XP-47B	LTT	8.7×10^6	NACA 66,2-115	80	10.4	0.0013	0.33	On	0.0001 ±0.00003	-------
									0		0.0005 ±0.00003	
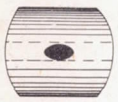	2	XP-63	LTT	5.2	NACA 66(2x15)-216	50	10.9	0.0028	0.28	On	0 ±0.00015	-------
	3						13.3	0.0034	0.23		0.0008 ±0.00015	
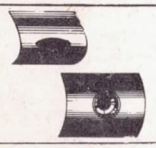	4	XP-41 (modified)	19-ft PT	6.15	NACA 66,2-018	35.5	4.7	0.0009	1.00	0.001c below	0 ±0.0001	0
	5						15.6	0.0035	0.26		0.0005 ±0.0001	
	6	XF4U-1	19-ft PT	2.8	NACA 23014	36	19.6	0.0043	0.25	On	0.0005 ±0.0002	0
	7											
	8	F4U-1	FST	7.6	NACA 23014	98	14.3	0.0023	----------	0.002c above	0 ±0.0002	0.07
	9											
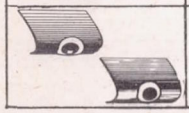	10	XF2A-2	FST	5.5	NACA 230(13.9)	71	21.6	0.0057	----------	0.005c above	0 ±0.0003	-0.06
	11									0.026c above	0.0007 ±0.0003	-0.01

[a]The abbreviations used apply to the following tunnels:

LTT, Langley two-dimensional low-turbulence tunnel
19-ft PT, Langley 19-foot pressure tunnel
FST, Langley full-scale tunnel
Ames 7 × 10, Ames 7- by 10-foot tunnel

[b]Based on Wing area = (Local chord)^2; one gun; estimated precision also given.

[c]Based on total wing area, all guns.

NATIONAL ADVISORY
COMMITTEE FOR AERONAUTICS

TABLE I.- GUN-PORT INSTALLATIONS - Concluded

Gun-port installation	Figure	Configuration	Source of data (a)	Reynolds number	Airfoil section	Wing chord (in.)	Gun-port height (percent t)	Entrance-area ratio, A_i/tc	Exit-area ratio, A_e/A_i	Gun-port position relative to chord line	Results	
											ΔC_{D_c} at $C_L = 0.2$ (b)	$\Delta C_{L_{max}}$ (c)
	12 13	Low-drag gun port	LTT	3.8×10^6	NACA 66(215)-213	36	25.0	0.027 .026 .019	0.56 .52 .49	On	0.0002 ±0.00005	-------
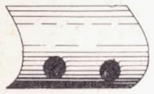	14 15 16	XA-41	Ames 7 × 10	6.35	NACA 64,3x-320	48	12.9	0.0031	0	0.016c below	0.0003 ±0.0001	-------
										0.008c below	0.0008 ±0.0001	
										On	0.0009 ±0.0001	
							16.5	0.0043	0	On and 0.005c above	0.0018 ±0.0001	
										0.005c and .010c above	0.0014 ±0.0001	
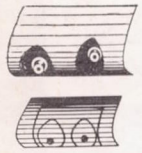	17 18	P-51B	FST	6.5	Compromise low drag 15.5 percent thick (minimum pressure at 0.4c)	83	26.2	Gun port open	----------	On	0.0003 ±0.0002	-0.12
							----------	Tape torn			0.0002 ±0.0002	-0.05
							5.8	0.0004			0.0001 ±0.0002	-0.02

[a]The abbreviations used apply to the following tunnels:

LTT, Langley two-dimensional low-turbulence tunnel
19-ft PT, Langley 19-foot pressure tunnel
FST, Langley full-scale tunnel
Ames 7 × 10, Ames 7- by 10-foot tunnel

[b]Based on Wing area = $(\text{Local chord})^2$; one gun; estimated precision also given.

[c]Based on total wing area, all guns.

NATIONAL ADVISORY
COMMITTEE FOR AERONAUTICS

TABLE II.- PROTRUDING MACHINE-GUN INSTALLATIONS

Protruding machine-gun installation	Figure	Configuration	Source of data (a)	Reynolds number	Airfoil section	Wing chord (in.)	Gun diameter (percent t)	Gun extension (percent c)	Machine-gun position relative to chord line	Results	
										ΔC_{D_c} at $C_L = 0.2$	$\Delta C_{L_{max}}$
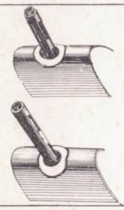	19 20	XP2A-2	FST	5.5×10^6	NACA 230(13.9)	72	21.8	2.8	0.026c above	0.0004 ±0.0003	-0.14
								13.9	0.026c above	0.0007 ±0.0003	------
								13.9	0.005c above	0.0003 ±0.0003	-0.13
								25.4	0.005c above	0.0004 ±0.0003	-0.09
	21 23	XP-41 (modified)	19-ft PT	6.2	NACA 66,2-018	35.5	11.7	10.0	0.002c below	0.0004 ±0.0001	0
	22 23	F6F-3	FST	8.0	NACA 23015	103	----------	3.9 (av.)	0.022c above (av.)	0.0001 ±0.0002	-0.05
	24 25	XP-63	TDT	6.0	NACA 66(215)-116, a = 0.6	24	13.8	19.1	On	0.0010 ±0.00004	------
	24 25	XP-63	TDT	6.0	NACA 66(215)-116, a = 0.6	24	13.8	19.1	0.110c underslung	0.0016 ±0.00006	------
	24 25	P-63A	FST	6.4	NACA 66(215)-116	72	13.8	19.1	0.110c underslung	[b]0.0038 ±0.0007 [c]0.0031 ±0.0007	0.01 ------
	26 27	XA-26	19-ft PT	3.6	NACA 65(216)-215, a = 0.8	22	13.3	6.4 -2.0	0.147c underslung	0.0026 ±0.0006	0
Sealed	28	F4F-3	Flight	-------	----------	106	----------	5.5 and 0	0.002c inboard 0.001c outboard above	----------	0
Unsealed											-0.26

[a]The abbreviations used apply to the following tunnels:

FST, Langley full-scale tunnel
19-ft PT, Langley 19-foot pressure tunnel
TDT, Langley two-dimensional low-turbulence pressure tunnel

[b]Unsealed.

[c]Sealed.

NATIONAL ADVISORY
COMMITTEE FOR AERONAUTICS

TABLE III.- WING-CANNON INSTALLATIONS

Wing-cannon installation	Remarks	Figure	Configuration	Source of data (a)	Reynolds number	Airfoil section	Wing chord (in.)	Root diameter of fairing (percent t)	Cannon extension (percent c)	δ_f (deg)	Cannon position relative to chord line	Results	
												ΔC_{D_c} at $C_L = 0.2$	$\Delta C_{L_{max}}$
	Fairing 1	29 30	XF2A-2	FST	5.5×10^6	NACA 230(13.9)	72	----------	Underslung	0	Approx. 0.10c below	0.0046 ±0.0007	-0.09
	Fairing 2											0.0038 ±0.0007	-0.05
	Submerged							69.1	49		On	0.0014 ±0.0007	-0.04
	---------	31 32	20-mm cannon	TDT	6.0	NACA 23015	24	26.0	16.5	0	0.006c below	0.0004 ±0.00002	------
						NACA 65,3-418		21.7				0.0006 ±0.00003	
						NACA 66(215)-216	36	24.4				0.0008 ±0.00004	
								38.2	34.1		0.012c below	0.0009 ±0.00004	
	Rough spot							----------	0		----------	0.0008 ±0.00004	
	Fairing A	33 36	XF14C-2	19-ft PT	5.5	N-71 16.2 percent thick	39.7	31.5	16.7 inboard and 24.9 outboard	0	Below	0.0005 ±0.0002	0
	Fairing B											0.0002 ±0.0002	0.02
										50		----------	-0.07
	Unfaired	34 36	XF6F	19-ft PT	6.15	NACA 65(318)-1(18.5)	39	10.3	5.4 inboard and 17.7 outboard	0	On	0.0005 ±0.0001	-0.08
										35		----------	-0.26
	Round fairing									0		0.0005 ±0.0001	0.04
										35		----------	-0.12
	Razorback fairing									0		0.0002 ±0.0001	0.02
										35		----------	-0.07

[a] The abbreviations used apply to the following tunnels:

FST, Langley full-scale tunnel
TDT, Langley two-dimensional low-turbulence pressure tunnel
19-ft PT, Langley 19-foot pressure tunnel
Ames 7 × 10, Ames 7- by 10-foot tunnel

TABLE III.- WING-CANNON INSTALLATIONS - Concluded

Wing-cannon installation	Remarks	Figure	Configuration	Source of data (a)	Reynolds number	Airfoil section	Wing chord (in.)	Root diameter of fairing (percent t)	Cannon extension (percent c)	δ_f (deg)	Cannon position relative to chord line	Results: ΔC_{D_c} at $C_L = 0.2$	Results: $\Delta C_{L_{max}}$
	Unfaired	35, 36	XF4U-1	19-ft PT	2.75×10^6	NACA 23014	36	43.6	28.4 inboard and 20.0 outboard	0	0.0014c below inboard and .0028c below outboard	0.0006 ±0.0002	0
										50		----------	-0.02
	Short fairing									0		0.0002 ±0.0002	0.04
										50		----------	0.03
	Long fairing									0		0.0002 ±0.0002	0.02
										50		----------	0.05
	$\frac{V_1}{V_o} = 0.57$	37, 38	XA-41	Ames 7 × 10	6.35	NACA 64,3x-320	48	----------	2.3	0	0.005c and .010c above	0.0007 ±0.0001	------
	$\frac{V_1}{V_o} = 0.30$											0.0007 ±0.0001	
	Short fairings, $\frac{V_1}{V_o} = 0.30$											0.0004 ±0.0001	
	Long fairings, $\frac{V_1}{V_o} = 0.57$											0.0008 ±0.0001	
	Shields, no fairings, no flow										On and 0.005c above	0.0010 ±0.0001	
												0.0006 ±0.0001	
	Short fairings, no flow										0.005c and .010c above	0.0008 ±0.0001	
	Long fairings, no flow											0.0008 ±0.0001	
	----------	39, 40	P-51B	FST	6.0	Low-drag section 15.5 percent thick (min. pressure, 0.4c)	83	70.0	45.4	0	On	0.0006 ±0.0002	-0.07
	----------	41, 43	F4U-1	FST	7.6	NACA 23014	98	36.4	30.4 inboard and 20.7 outboard	0	0.012c and .008d below	0.0002 ±0.0003	-0.06
	----------	42, 43	F6F-3	FST	8.0	NACA 23015	103	----------	See picture	0	----------	0.0004 ±0.0003	------

[a]The abbreviations used apply to the following tunnels:

FST, Langley full-scale tunnel
TDT, Langley two-dimensional low-turbulence pressure tunnel
19-ft PT, Langley 19-foot pressure tunnel
Ames 7 × 10, Ames 7- by 10-foot tunnel

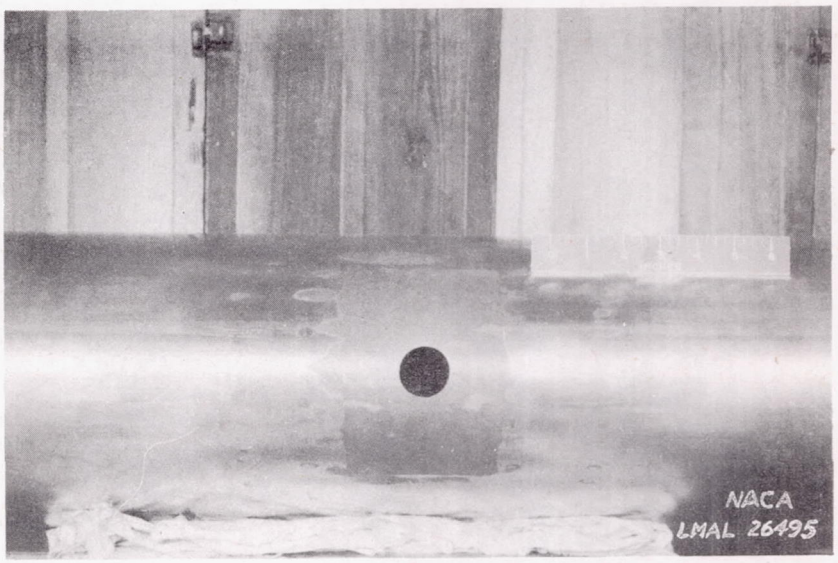

Figure 1.- Gun port on model of wing of XP-47B airplane. Gun-port diameter, 10.4 percent t.

CONFIDENTIAL

CONFIDENTIAL

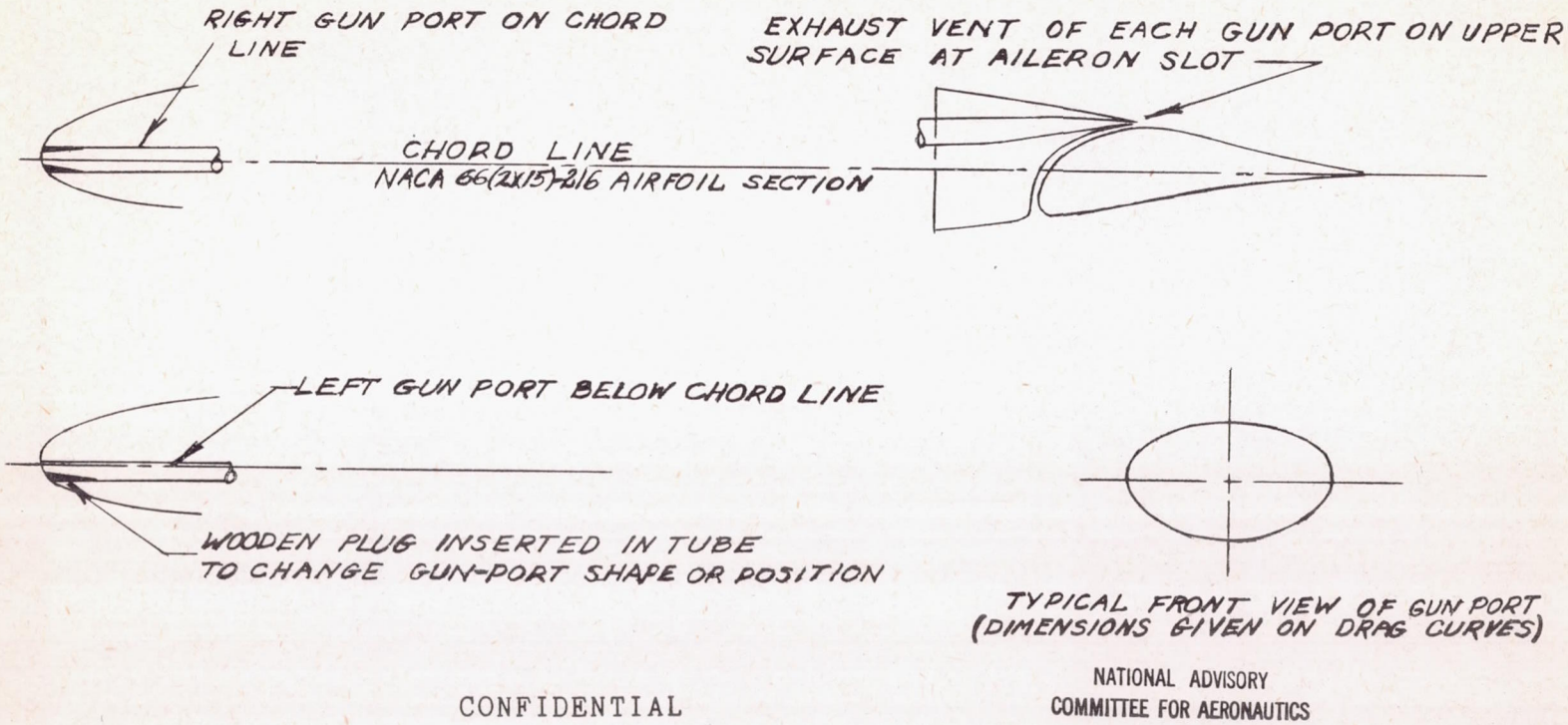

CONFIDENTIAL

Figure 2.- Gun-port installations on model of wing of XP-63 airplane.

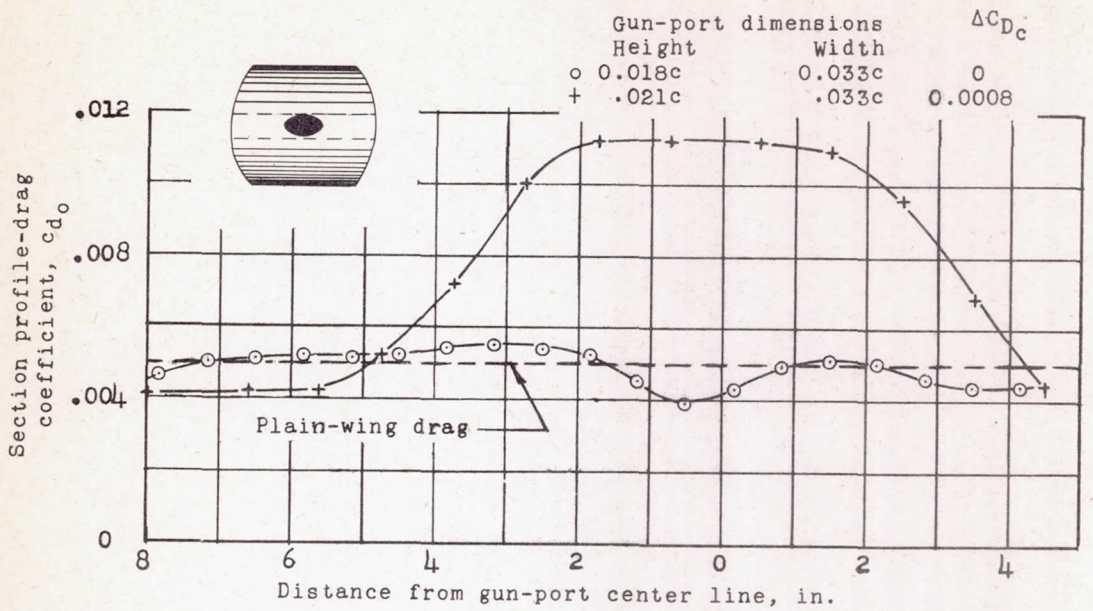

(a) Gun ports on chord line.

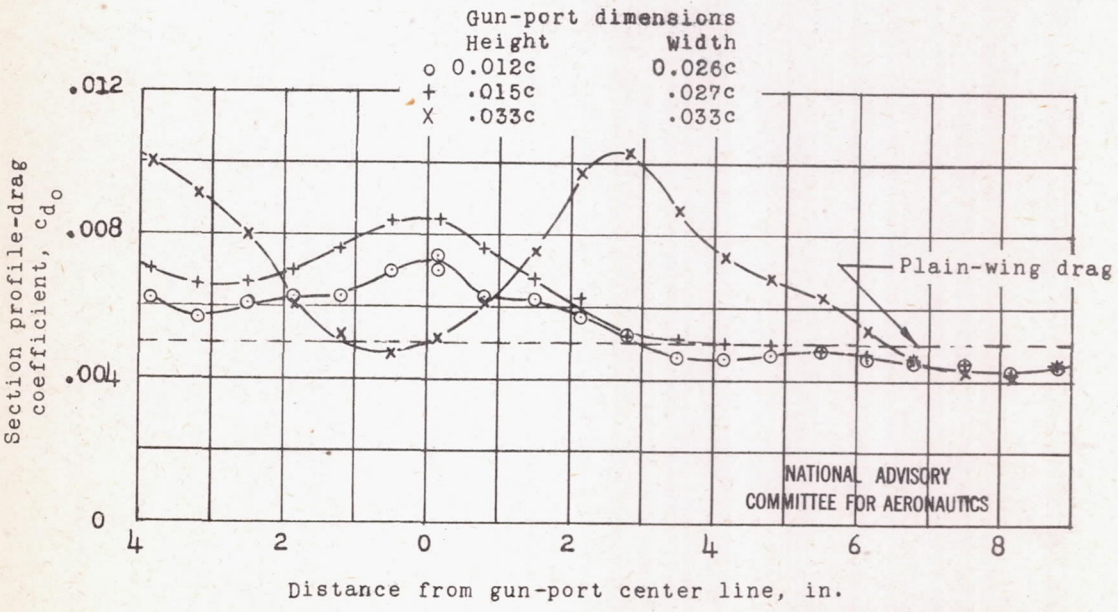

(b) Gun ports 0.014c below chord line.

CONFIDENTIAL

Figure 3.- Spanwise drag variation of several gun-port installations on model of wing of XP-63 airplane. c_l = 0.16; R = 5.2 X 10^6.

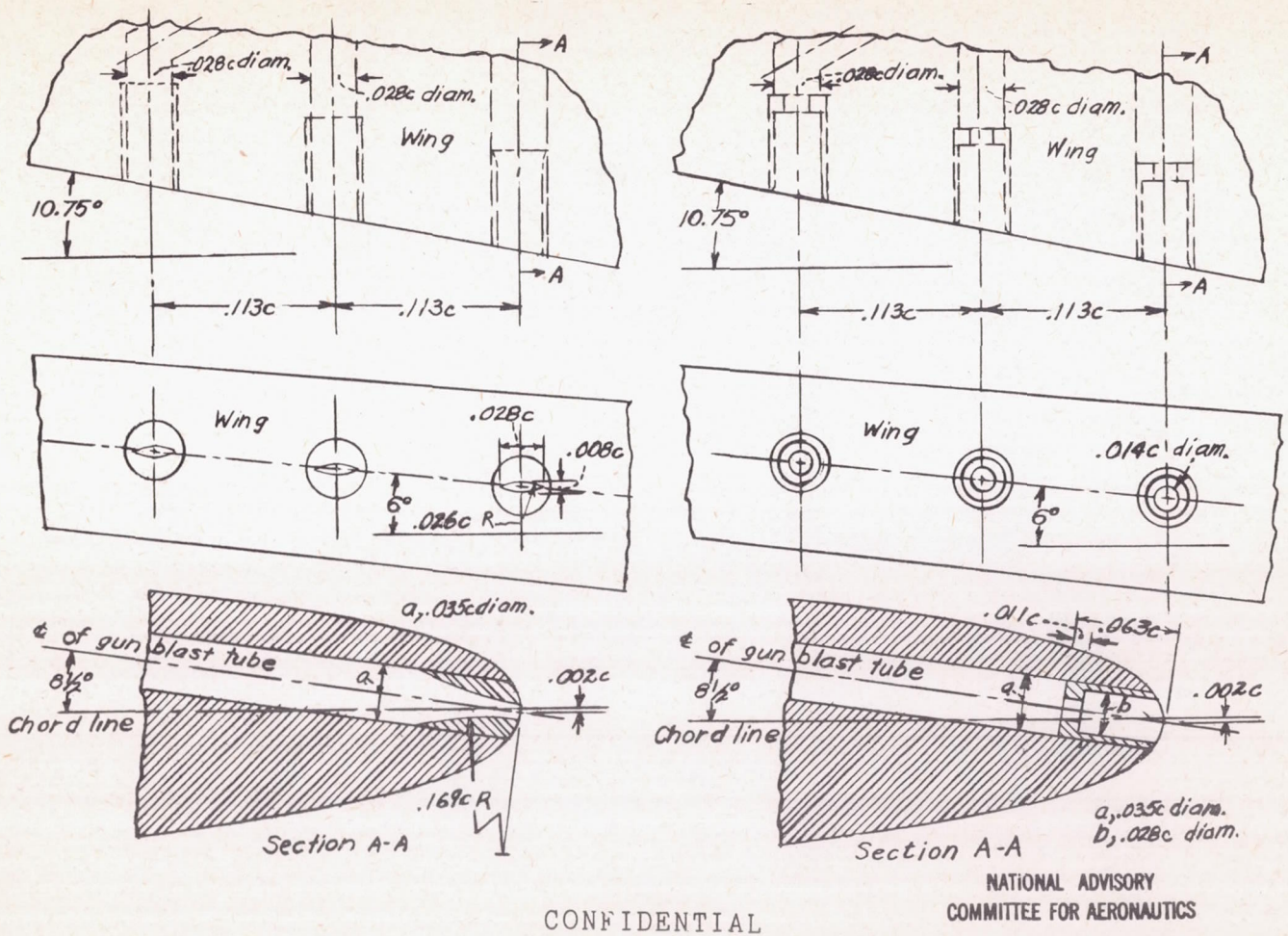

Figure 4.- Gun-port installations on wing of model of modified XP-41 airplane.

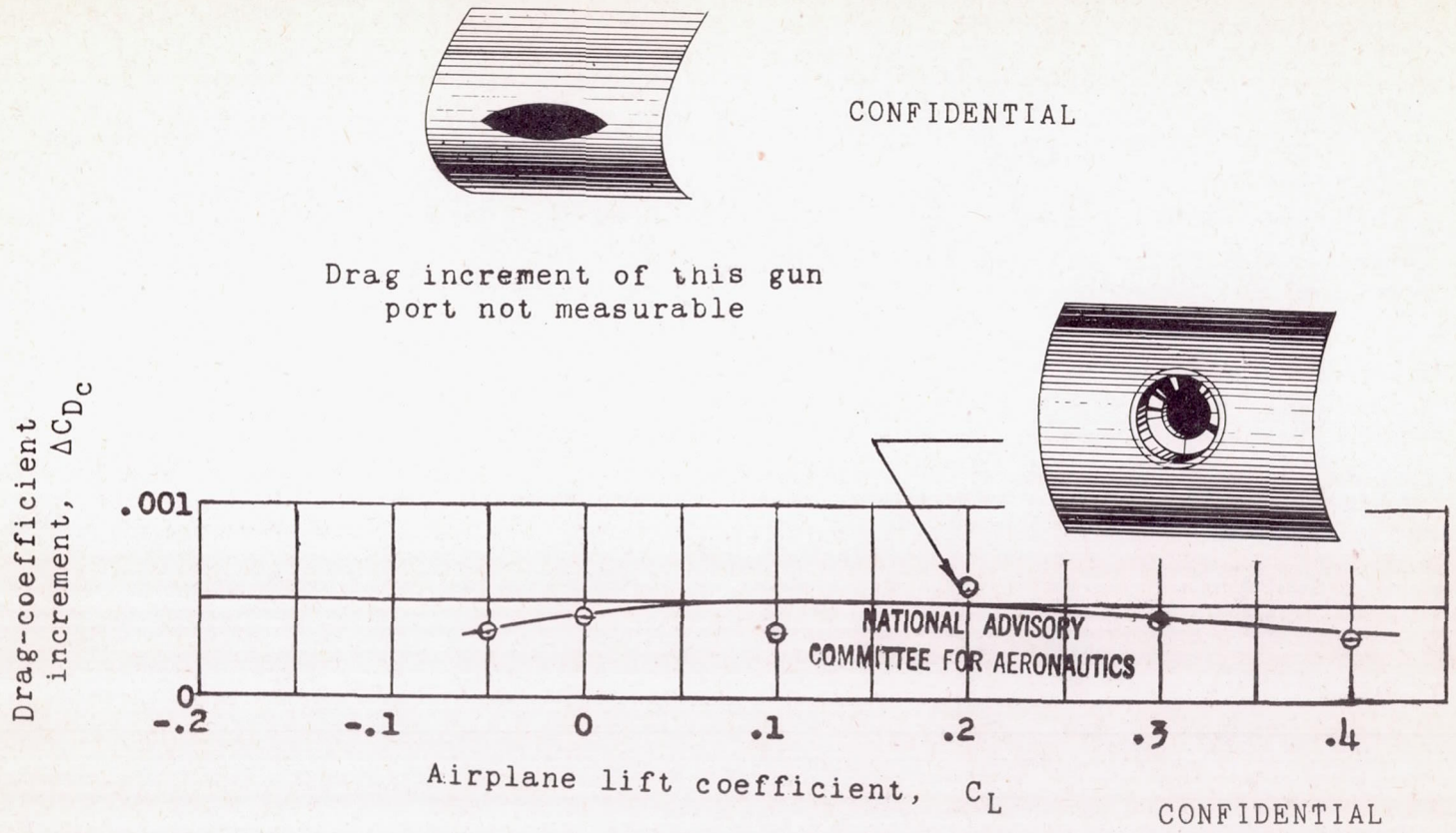

Figure 5.- Drag increments of gun ports on wing of model of modified XP-41 airplane in Langley 19-foot pressure tunnel. $R = 6.15 \times 10^6$.

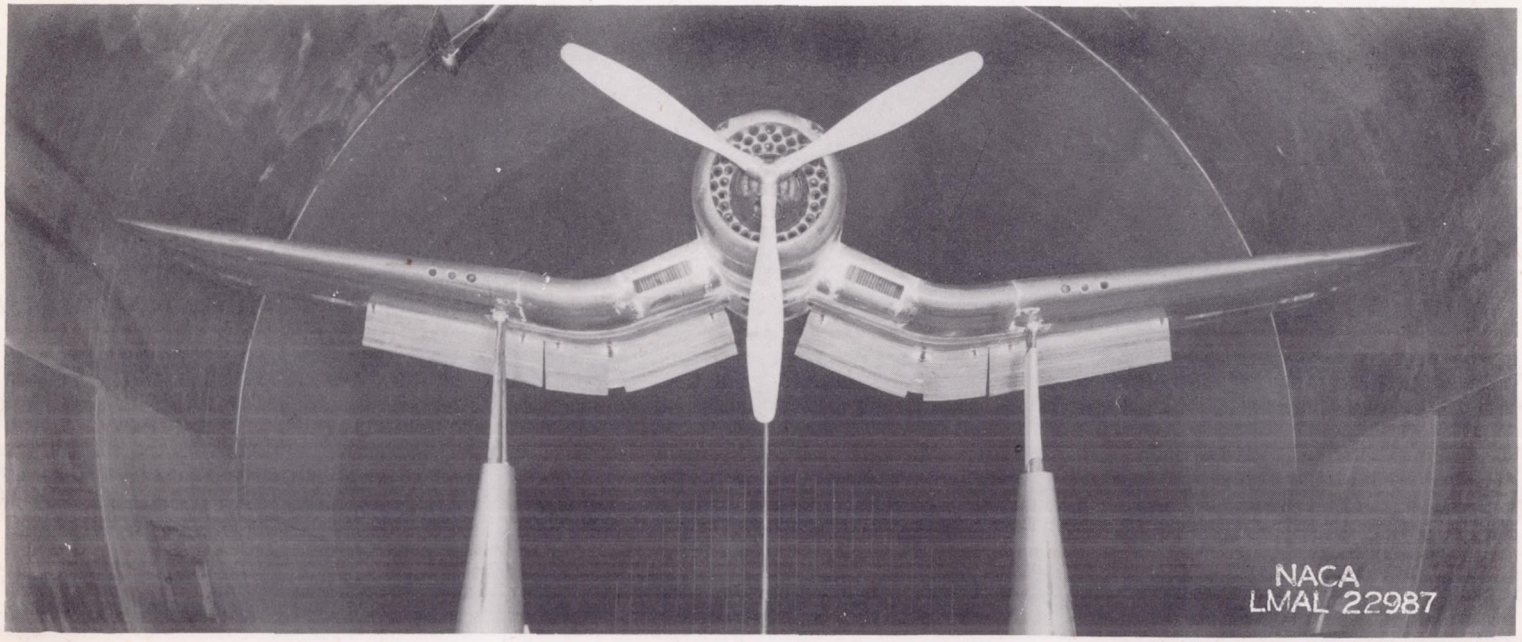

Figure 6.- Gun ports on $\frac{1}{2.75}$-scale model of XF4U-1 airplane.
Gun ports are of 1-inch diameter with exits ahead of flap.

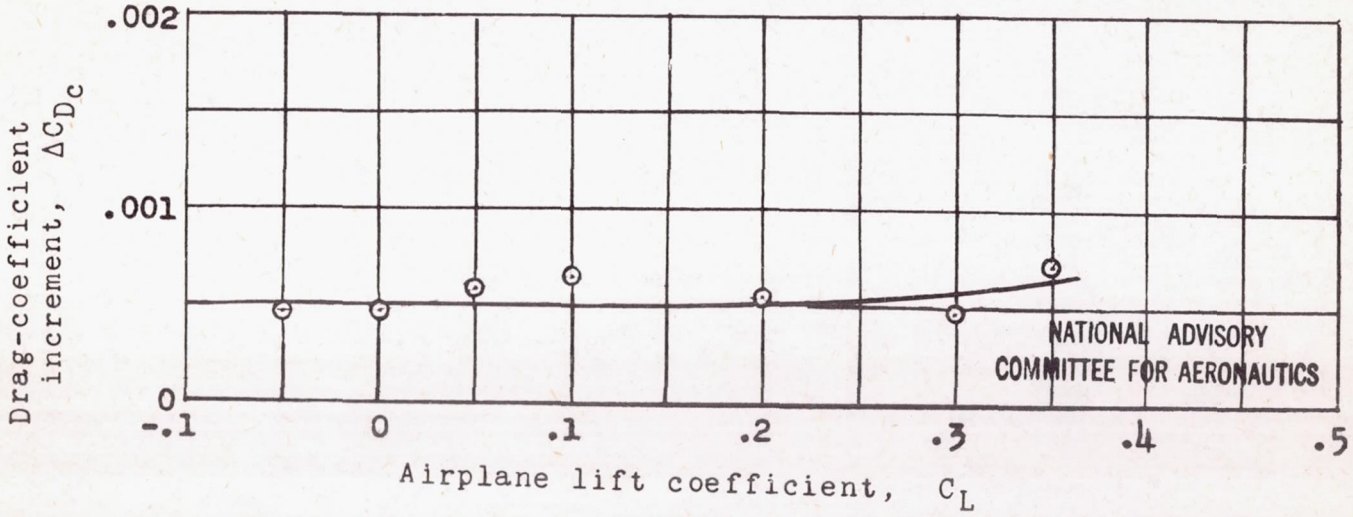

Figure 7.- Drag increments of gun ports on wing of model of XF4U-1 airplane in Langley 19-foot pressure tunnel. $R = 2.8 \times 10^6$.

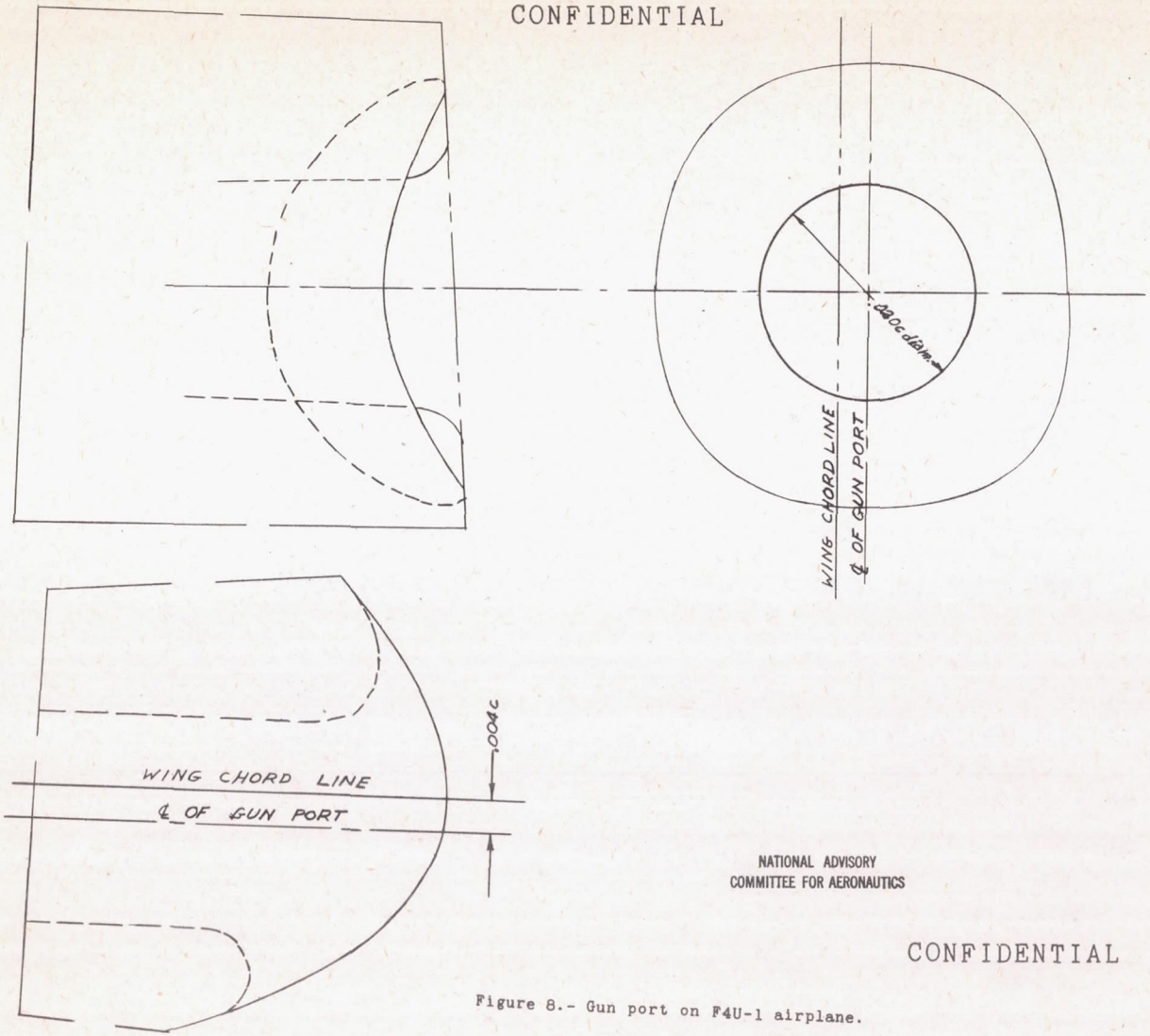

NATIONAL ADVISORY
COMMITTEE FOR AERONAUTICS

Figure 8.- Gun port on F4U-1 airplane.

CONFIDENTIAL

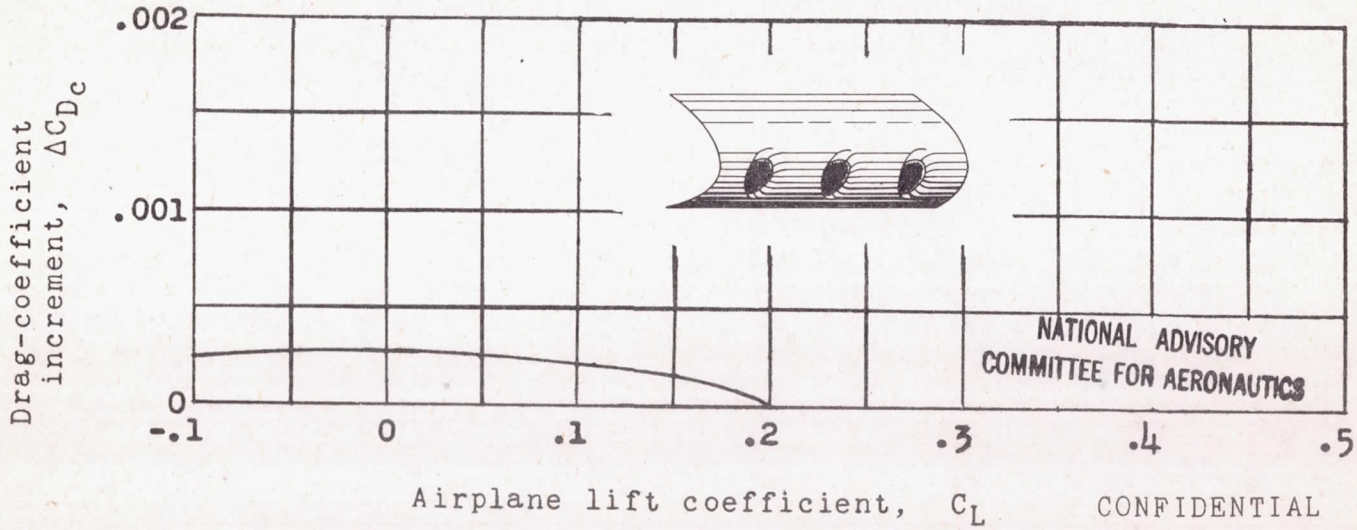

Figure 9.- Drag increments of gun ports on wing of F4U-1 airplane in Langley full-scale tunnel. $R = 7.6 \times 10^6$.

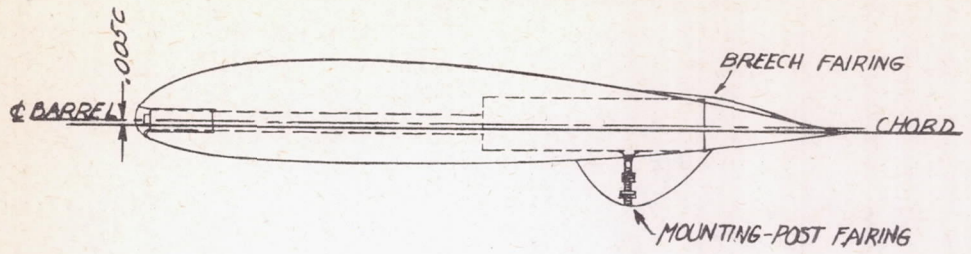

(a) Low flush gun position.

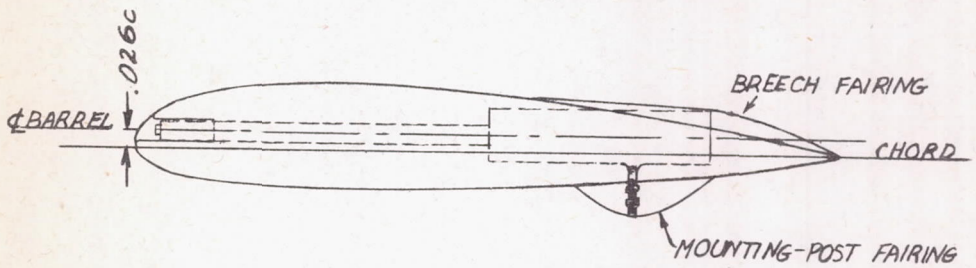

(b) High flush gun position.

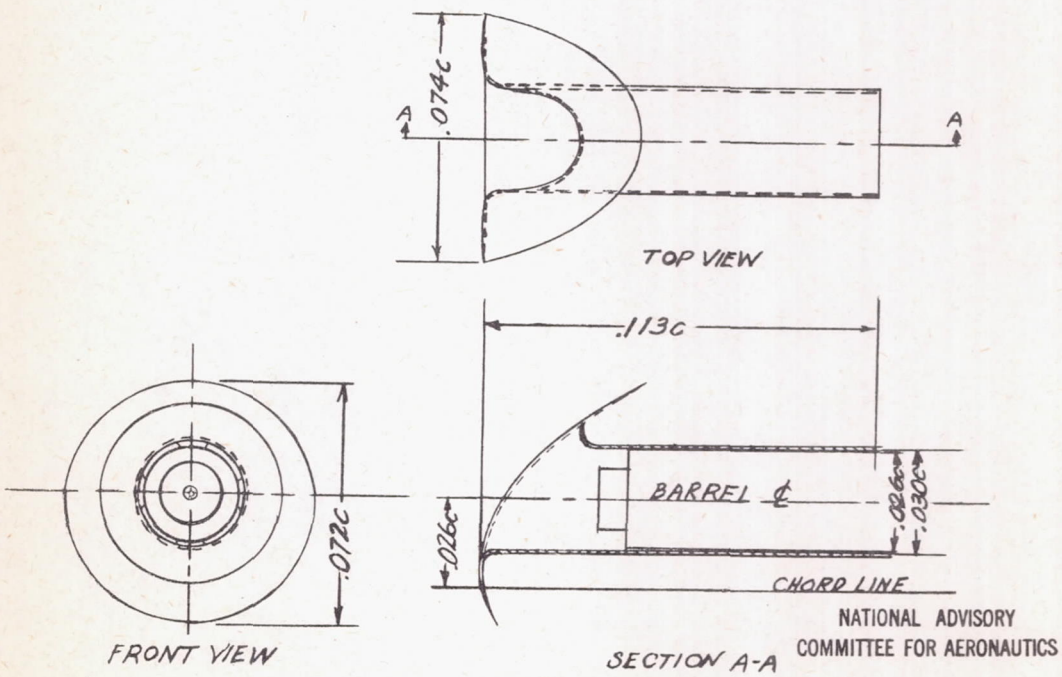

(c) Typical gun sleeve.

Figure 10.- Details of gun mounts on XF2A-2 airplane.

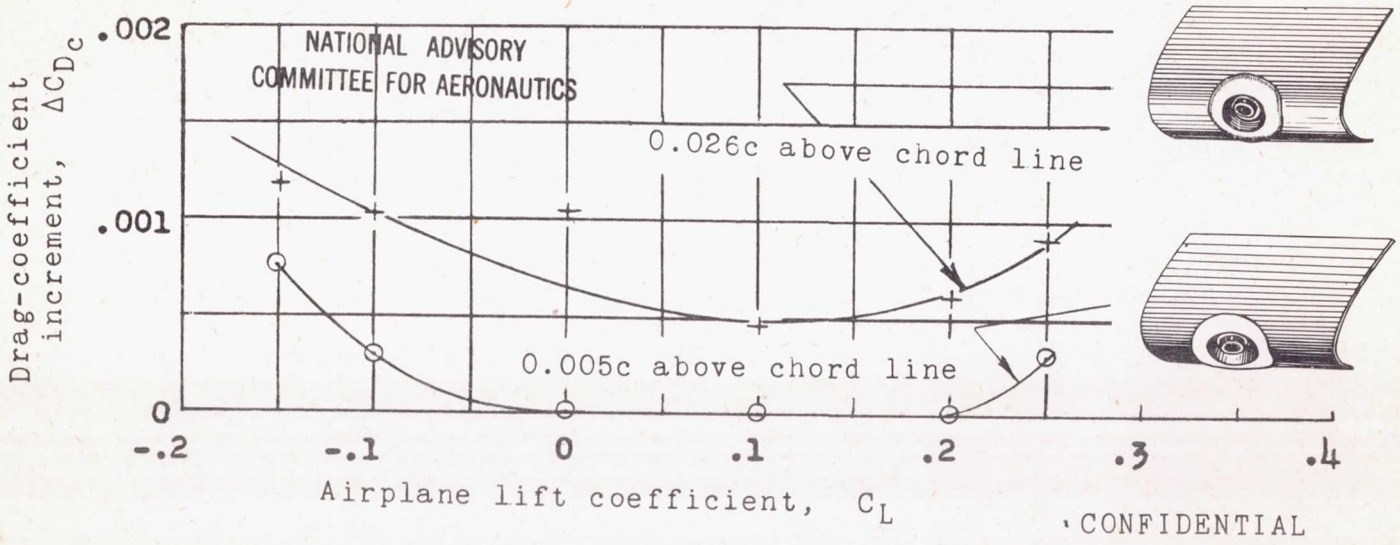

Figure 11.- Drag increments of gun ports on wing of XF2A-2 airplane in Langley full-scale tunnel. $R = 5.5 \times 10^6$.

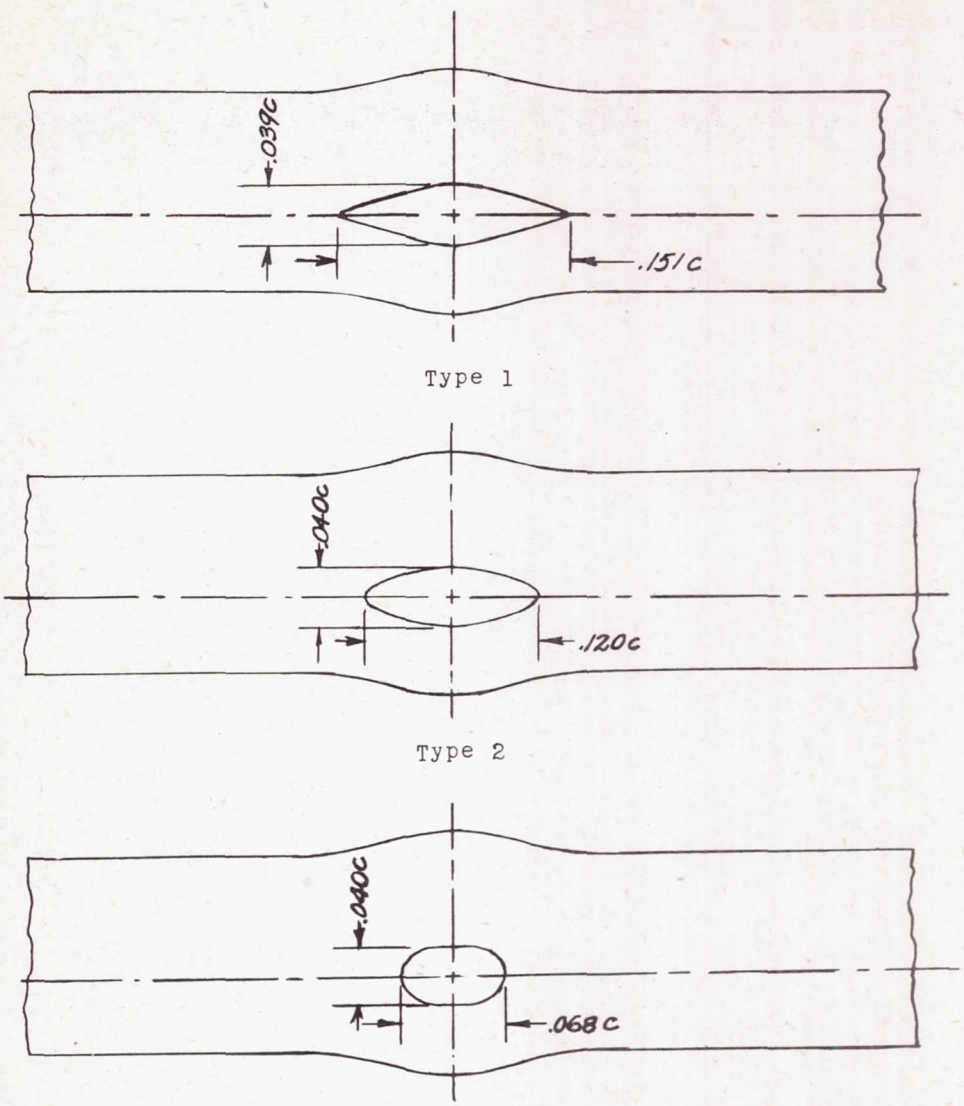

CONFIDENTIAL

(a) Front view of three types of opening.

Figure 12.- Details of openings of low-drag gun port.

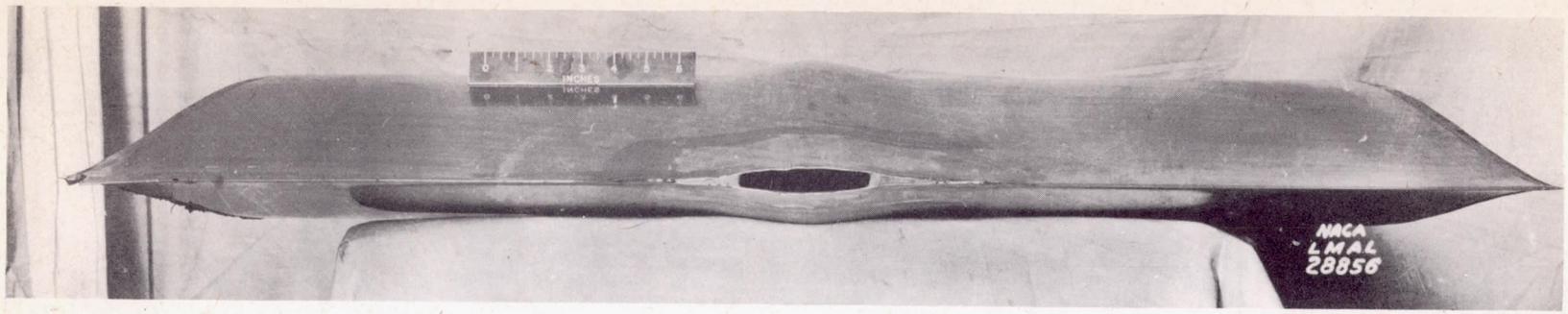

Rear view.

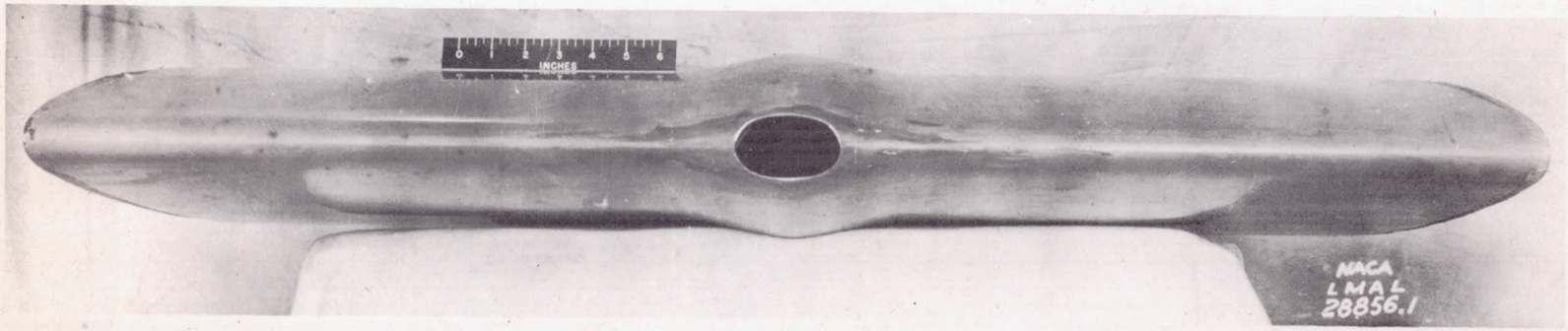

Front view.

(b) Type 3 opening.

Figure 12.- Concluded.

CONFIDENTIAL

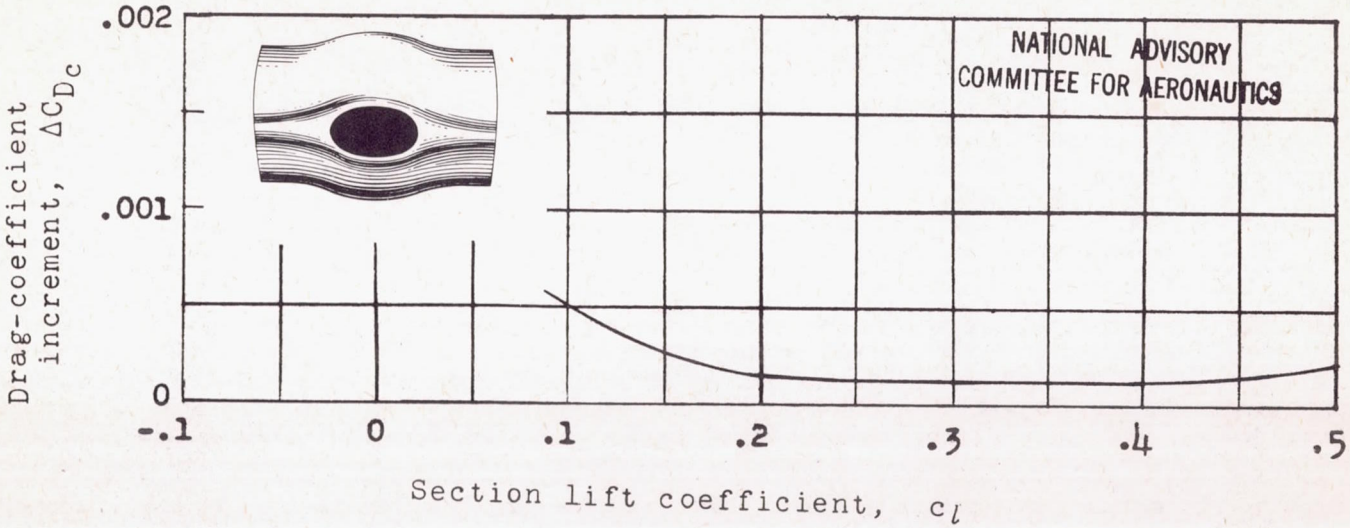

CONFIDENTIAL

Figure 13.- Drag increments of low-drag gun port in Langley two-dimensional low-turbulence tunnel. $R = 3.8 \times 10^6$.

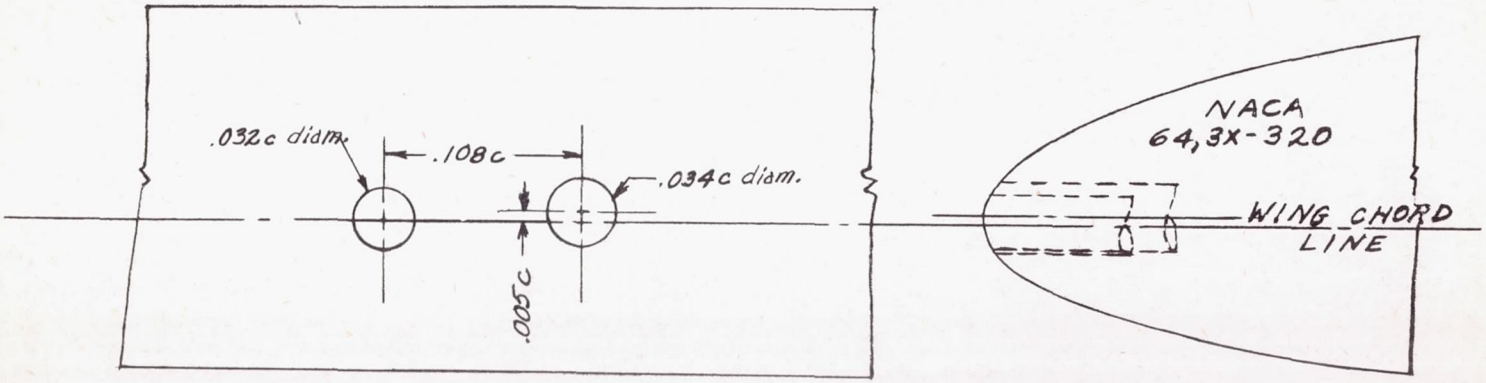

Figure 14.- Cannon ports on model of wing of XA-41 airplane. (This arrangement also tested with 0.032c diam. holes 0.005c above chord and 0.034c diam. holes 0.010c above chord.)

NATIONAL ADVISORY
COMMITTEE FOR AERONAUTICS

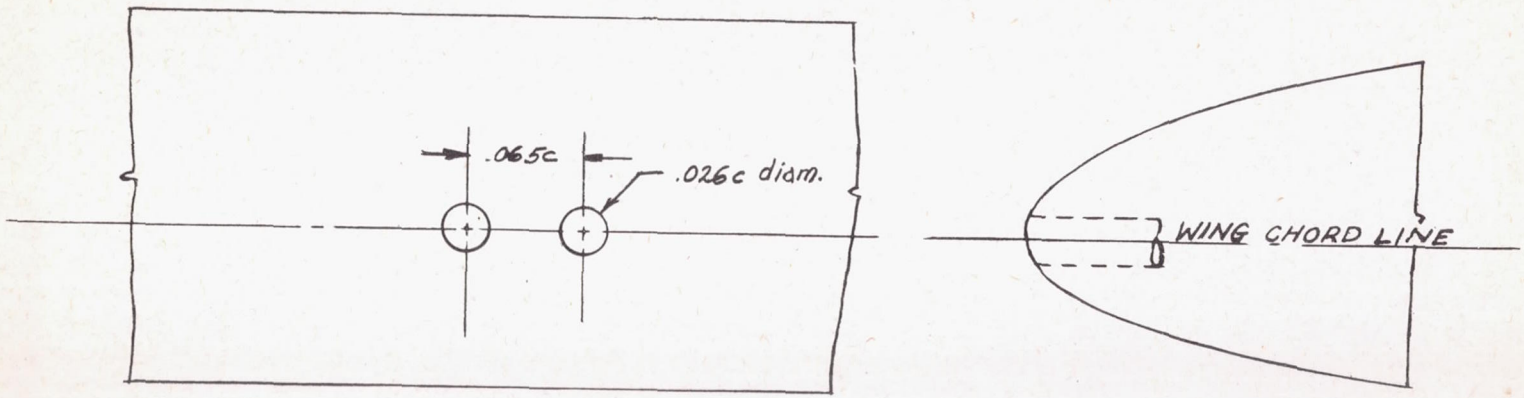

Figure 15.- Machine-gun ports on model of wing of XA-41 airplane. (These holes also tested centered 0.0082c and 0.0165c below chord.)

NATIONAL ADVISORY
COMMITTEE FOR AERONAUTICS

	Hole diam.	Position relative to chord line
o	0.026c	0.016c below
+	.026c	.008c below
X	.026c	On
□	.033c	On and .005c above
◇	.033c	.005c and .010c above

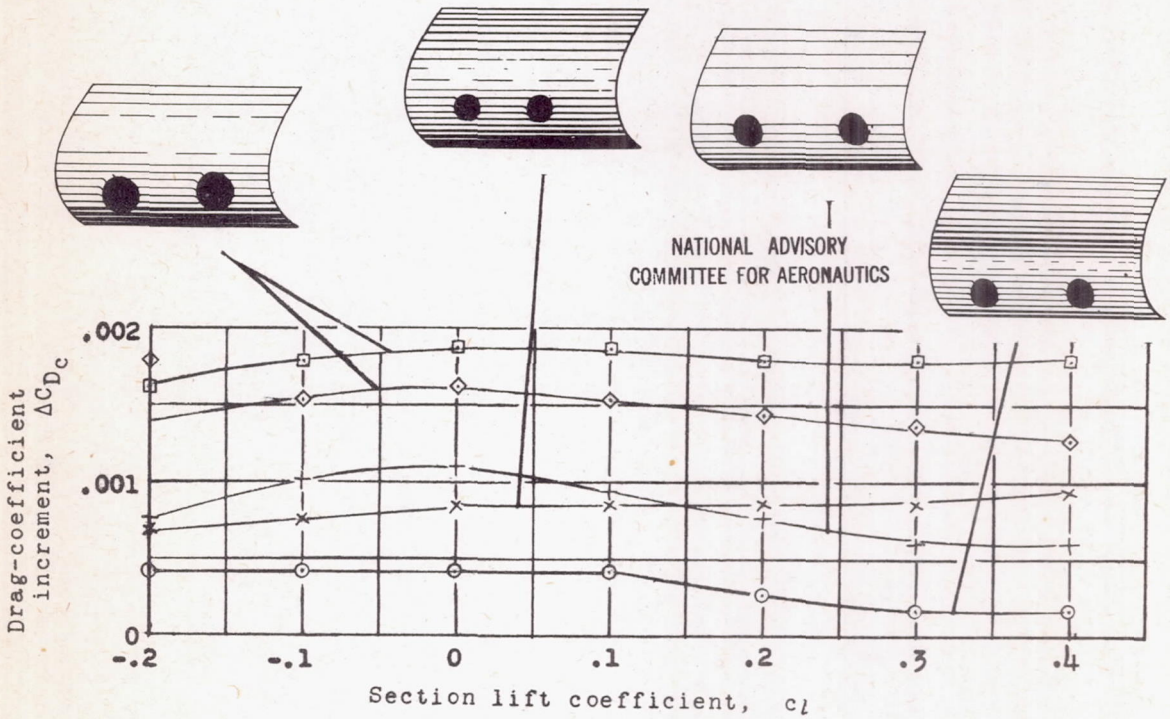

Figure 16.- Drag increments of gun ports on model of wing of XA-41 airplane in Ames 7- by 10-foot tunnel. No flow through ports. R = 6.35 X 10^6.

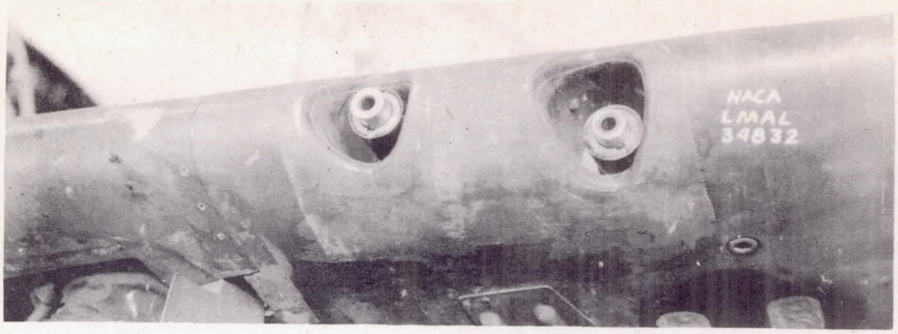

(a) Gun ports open.

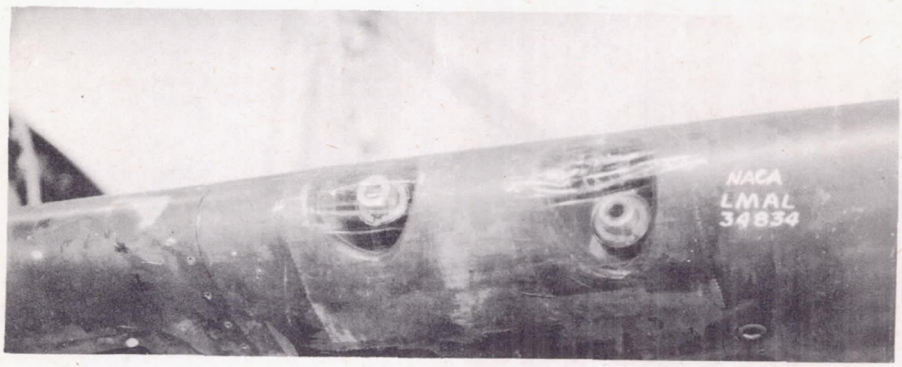

(b) Gun ports sealed with tape.

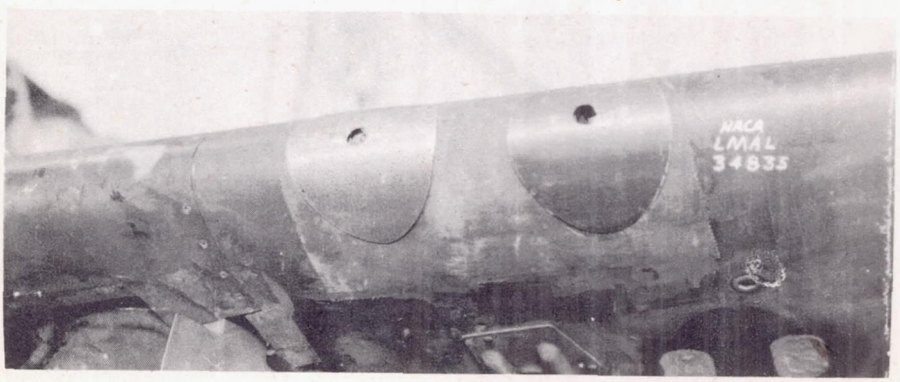

(c) Gun ports covered with metal plates having holes of 5.3-percent thickness to allow passage of bullet.

Figure 17.- Gun ports on P-51B airplane.

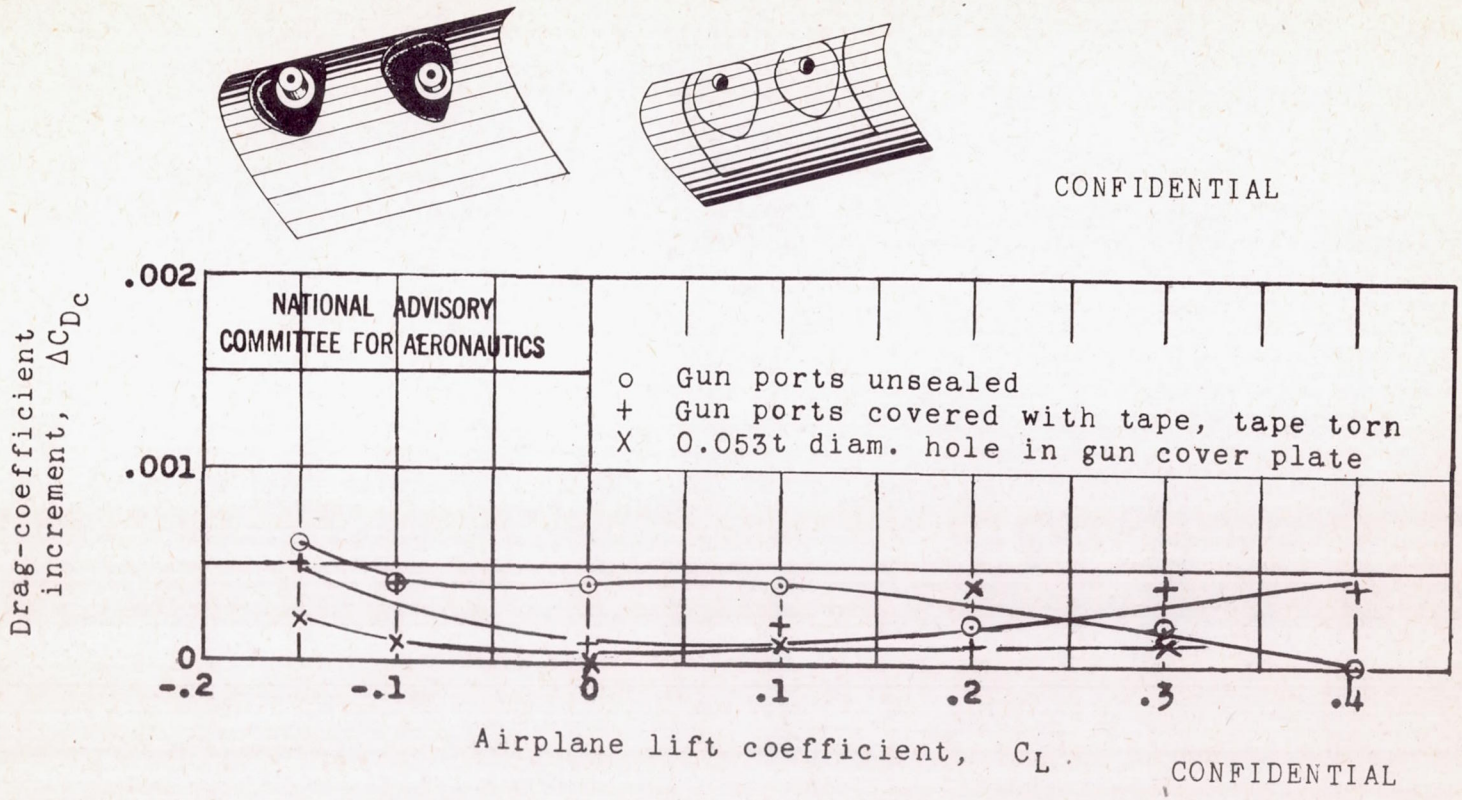

Figure 18.- Drag increments of several gun-port installations on P-51B airplane in Langley full-scale tunnel. $R = 6.5 \times 10^6$.

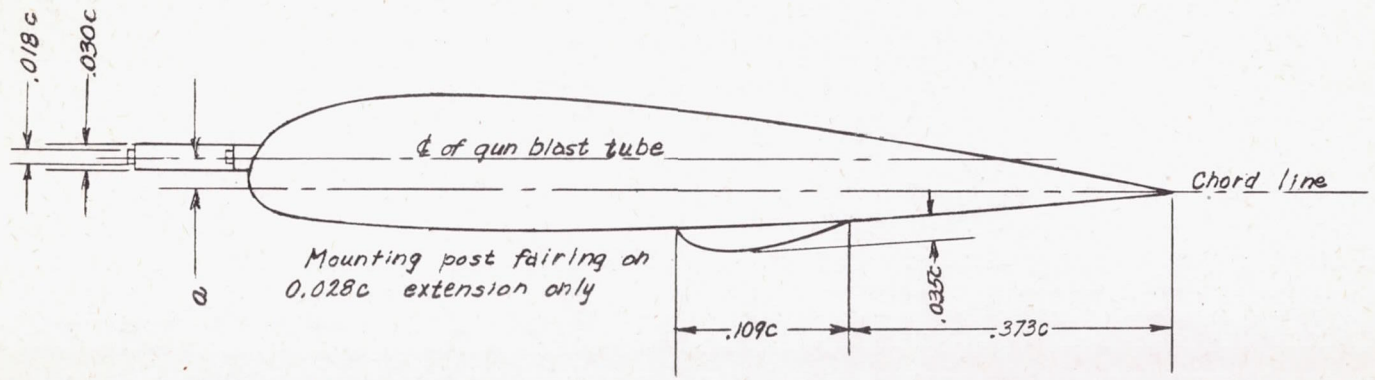

NATIONAL ADVISORY
COMMITTEE FOR AERONAUTICS

Figure 19.- Machine-gun extensions on XF2A-2 airplane. a = 0.026c or 0.005c; 0.254c gun extension not shown.

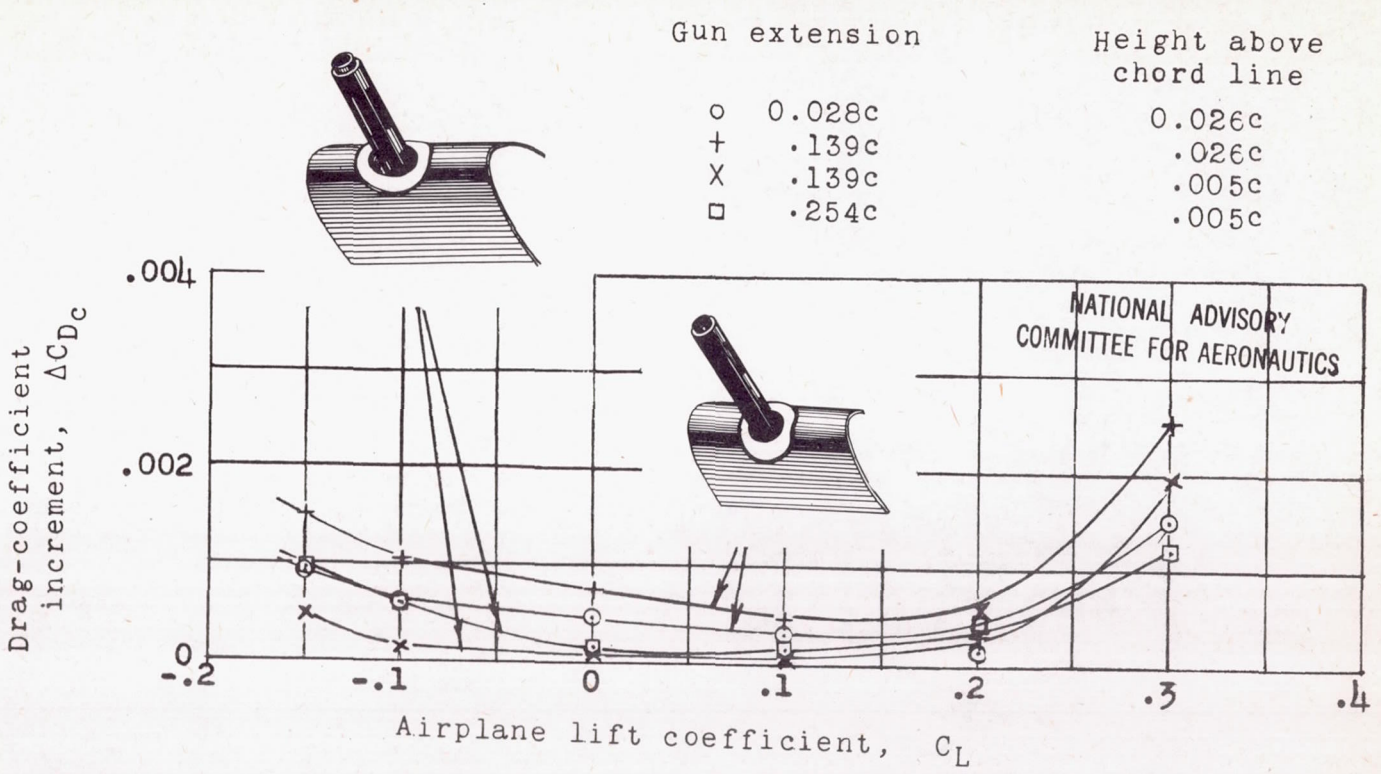

Figure 20.- Drag increments of machine-gun installations on XF2A-2 airplane in Langley full-scale tunnel. $R = 5.5 \times 10^6$.

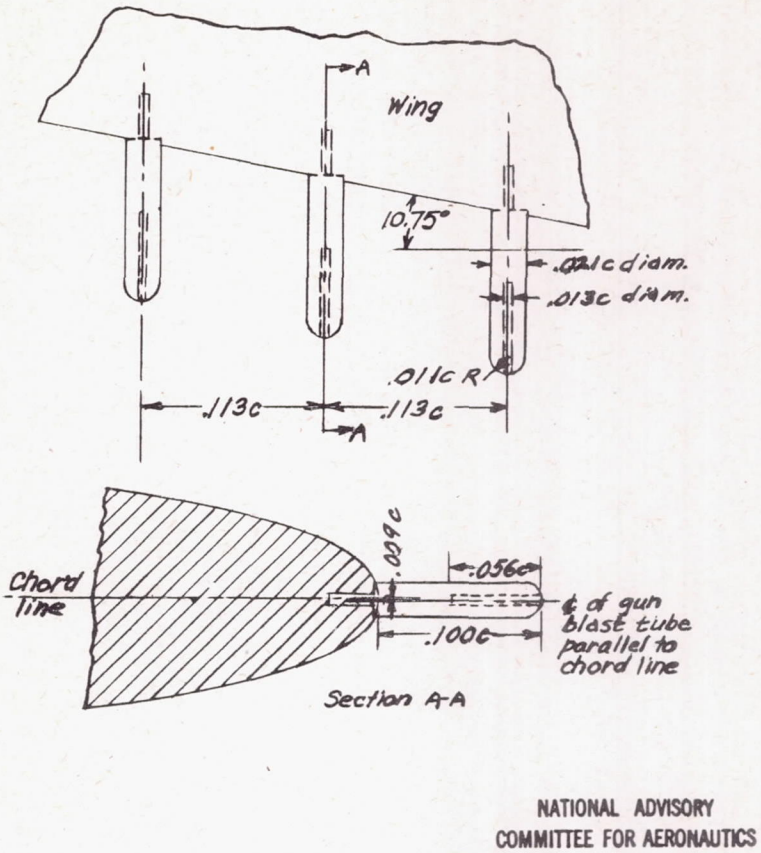

Figure 21.- Machine-gun installation on model of modified XP-41 airplane.

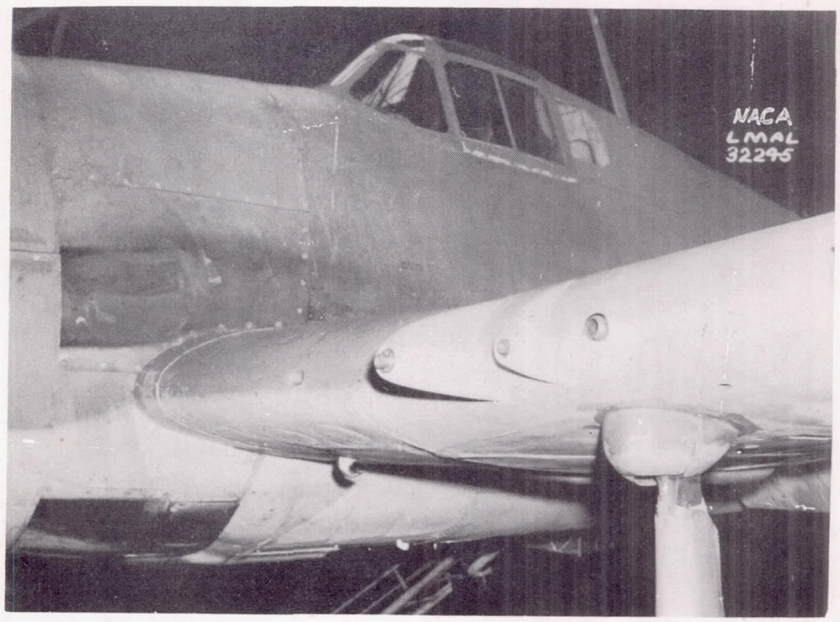

Figure 22.- Service gun fairings on F6F-3 airplane.

CONFIDENTIAL

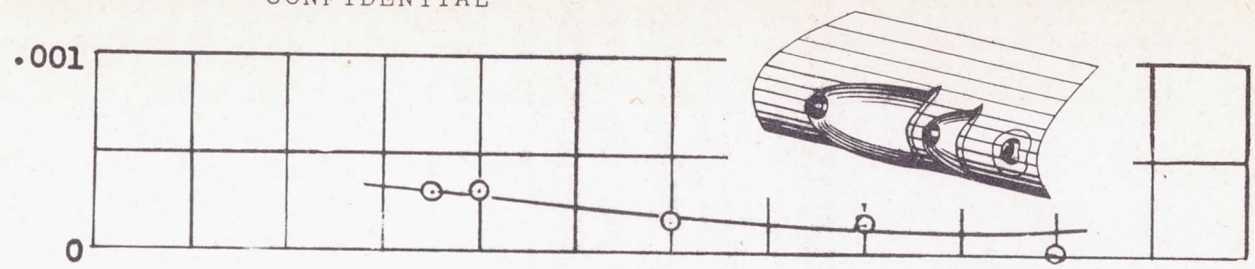

(a) Service gun fairings on F6F-3 airplane in Langley full-scale tunnel. $R = 8.0 \times 10^6$.

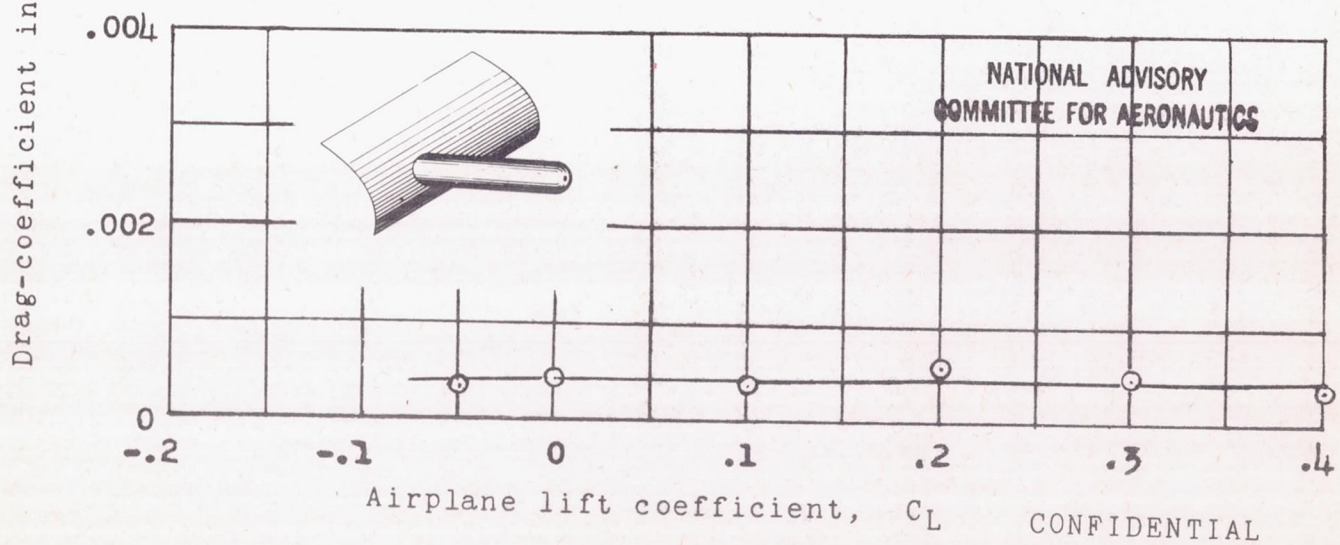

(b) Machine-gun installations on model of modified XP-41 airplane in Langley 19-foot pressure tunnel. $R = 6.2 \times 10^6$.

Figure 23.- Drag increments of two machine-gun installations.

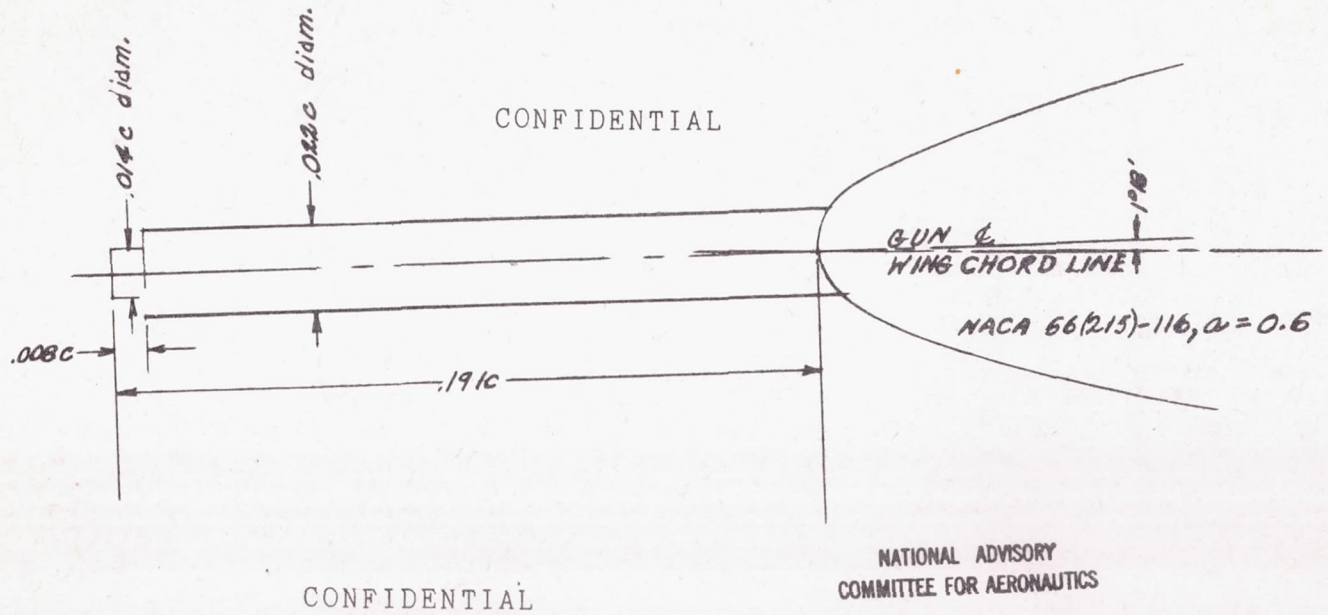

(a) Gun mounted on chord line of model of wing of XP-63 airplane.

Figure 24.- Machine-gun installations for XP-63 airplane.

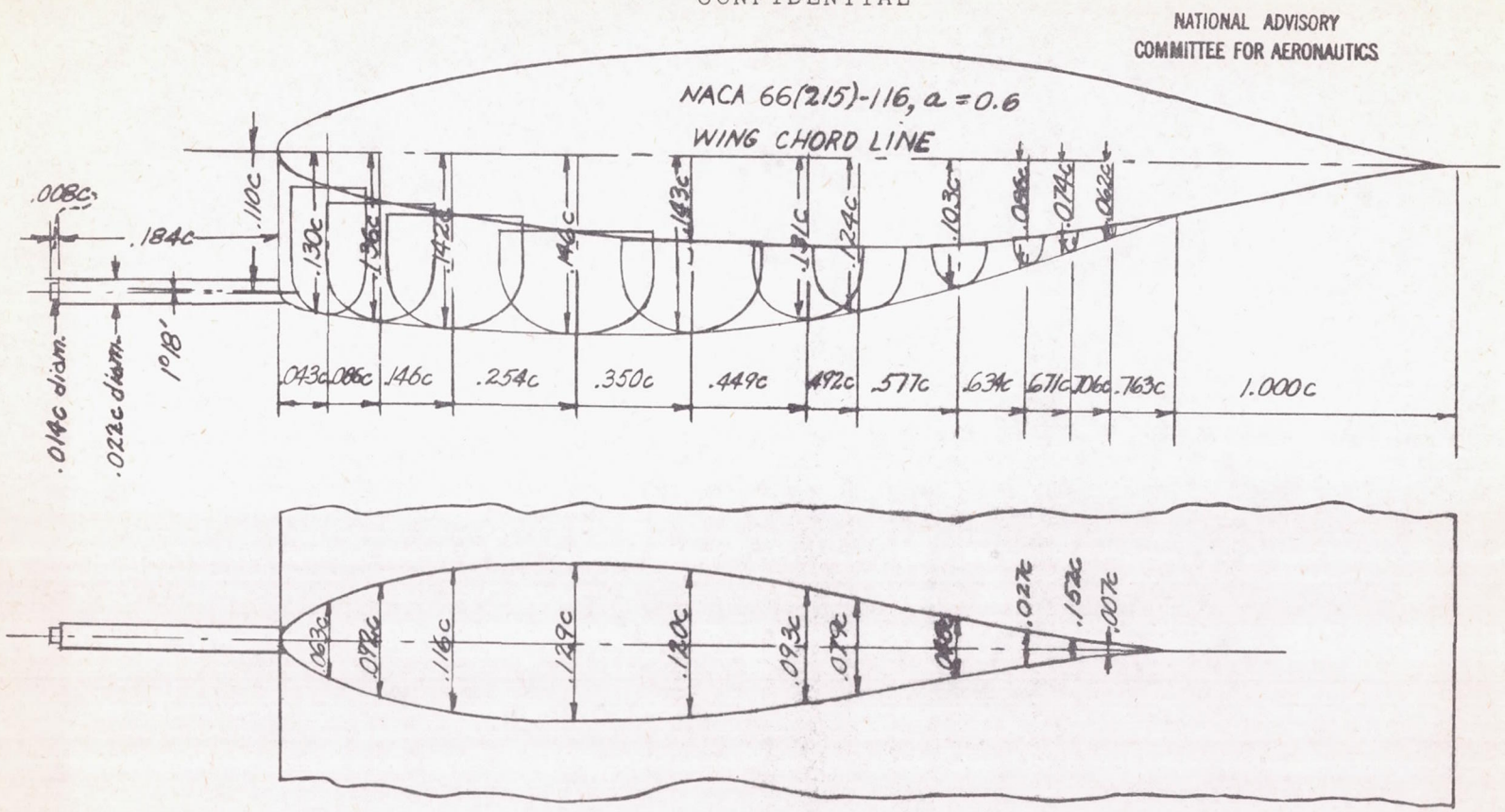

(b) Machine-gun mount on model of XP-63 wing and on P-63A airplane.

Figure 24.- Concluded.

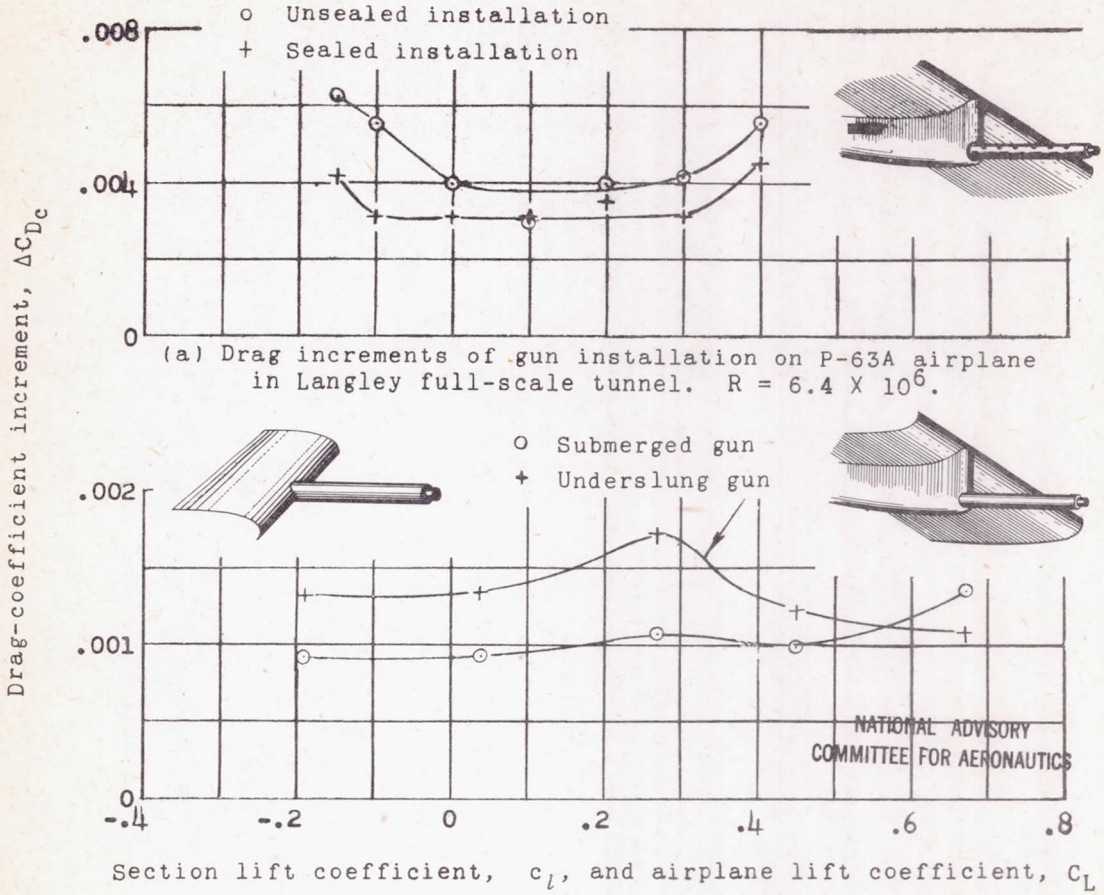

(a) Drag increments of gun installation on P-63A airplane in Langley full-scale tunnel. $R = 6.4 \times 10^6$.

(b) Drag increments of two gun installations on model of wing of XP-63 airplane in Langley two-dimensional low-turbulence pressure tunnel. $R = 6.0 \times 10^6$.

Figure 25.- Drag increments of machine-gun installations on model of wing of XP-63 airplane and on P-63A airplane.

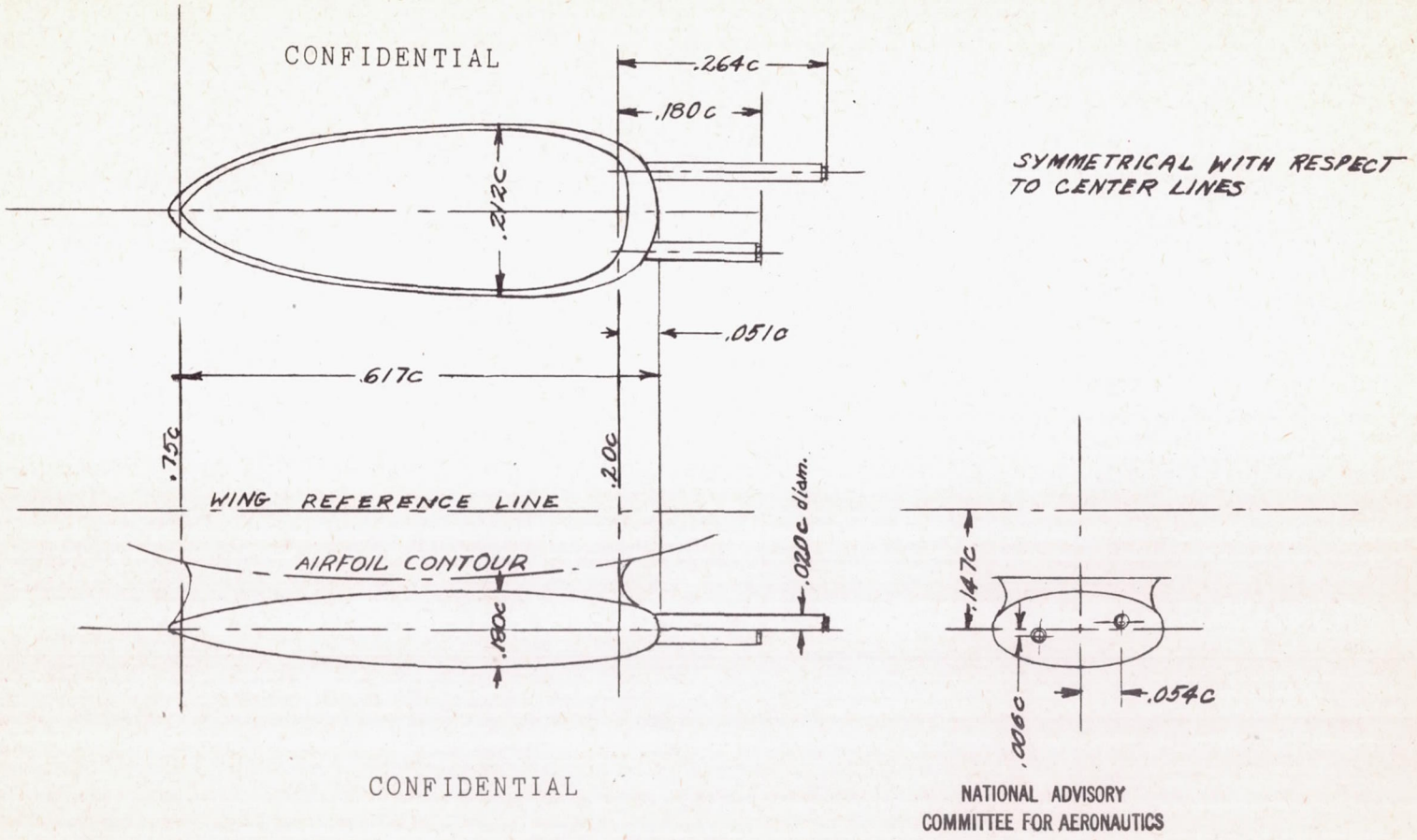

Figure 26.- Machine-gun mount on model of XA-26 airplane.

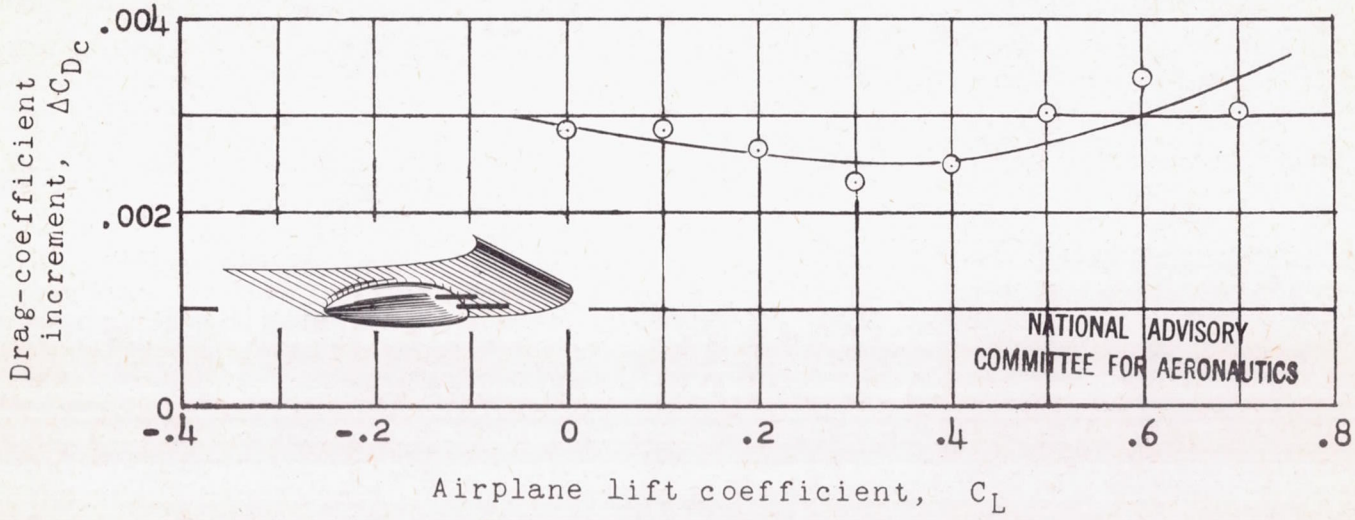

Figure 27.- Drag increments of gun installation on model of XA-26 airplane in Langley 19-foot pressure tunnel. $R = 3.6 \times 10^6$.

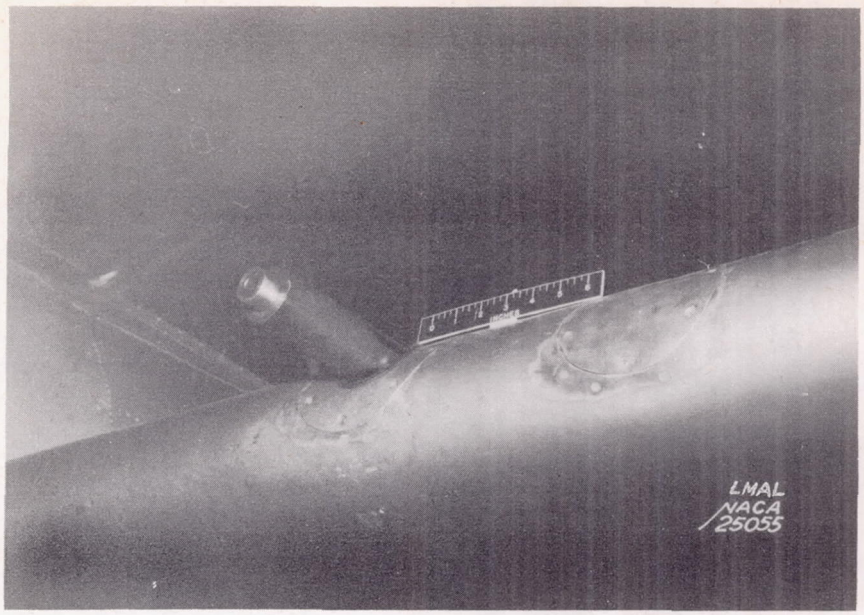

(a) View of projecting gun in unfaired condition with submerged gun removed.

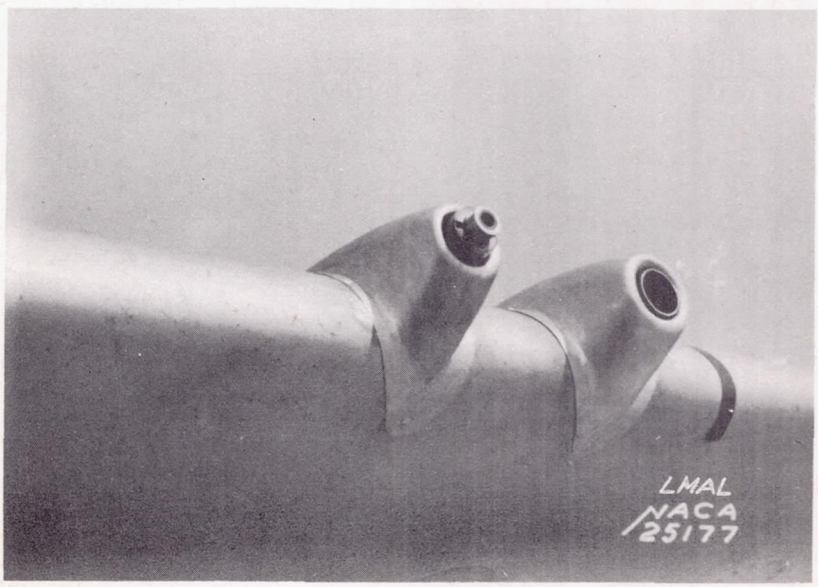

(b) View of fairing 1 on submerged gun and Grumman fairing on projecting gun. Both fairings provide space around gun barrel for cooling air.

Figure 28.- Gun fairings on F4F-3 airplane. (From reference 6.)

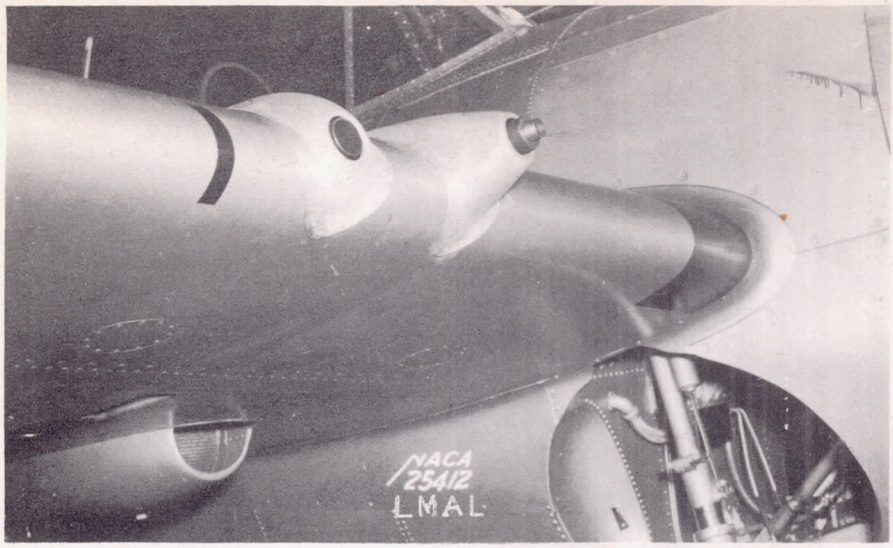

(c) View of fairing 2 (wide) on submerged gun and Grumman fairing on projecting gun. Both fairings provide space around gun barrel for cooling air.

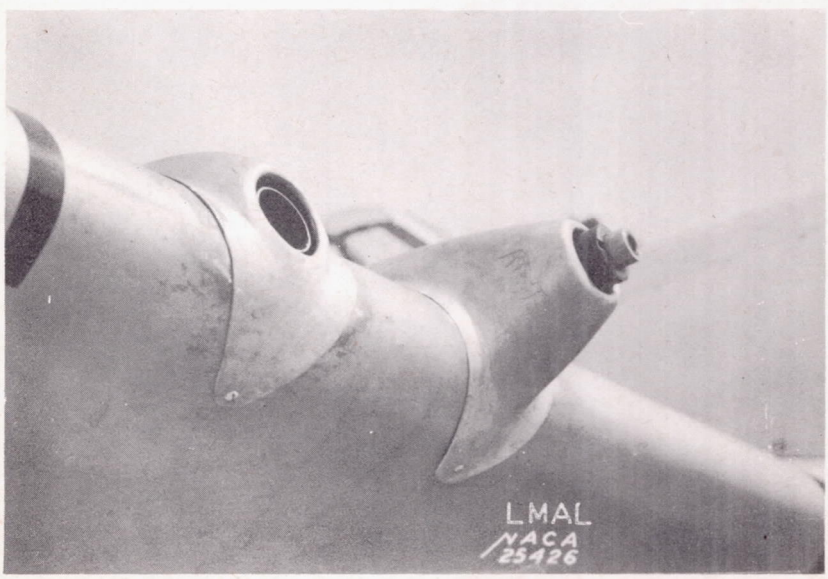

(d) View of fairing 3 (narrow) on submerged gun and Grumman fairing on projecting gun. Both fairings provide space around gun barrel for cooling air.

Figure 28.- Continued.

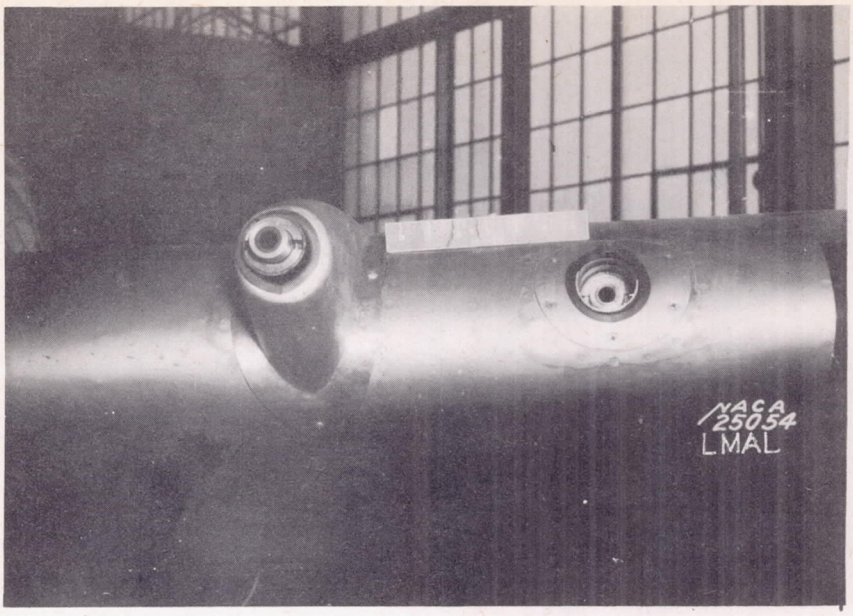

(e) View of submerged gun in unfaired condition and projecting gun with Grumman fairing. Rubber grommets installed around edges of fairing and wing opening.

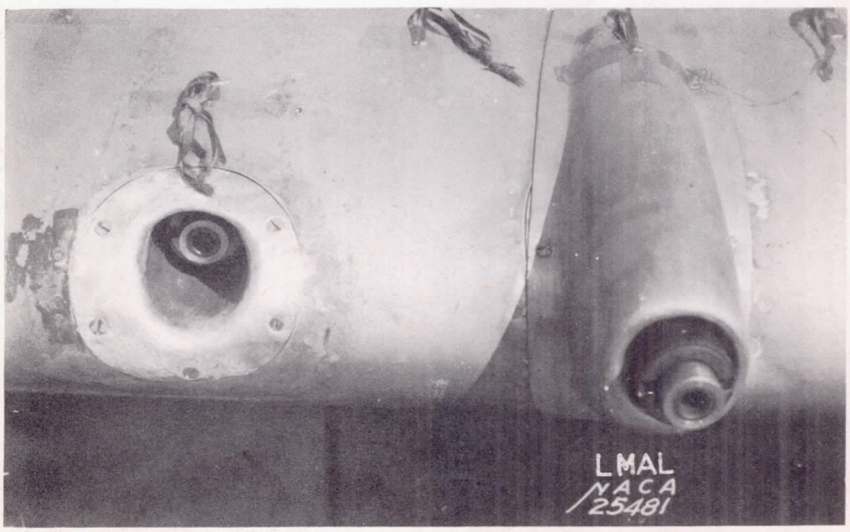

(f) View of faired wing opening for submerged gun and Grumman fairing on projecting gun. Both fairings provide space around gun barrels for cooling air.

CONFIDENTIAL

Figure 28.- Concluded.

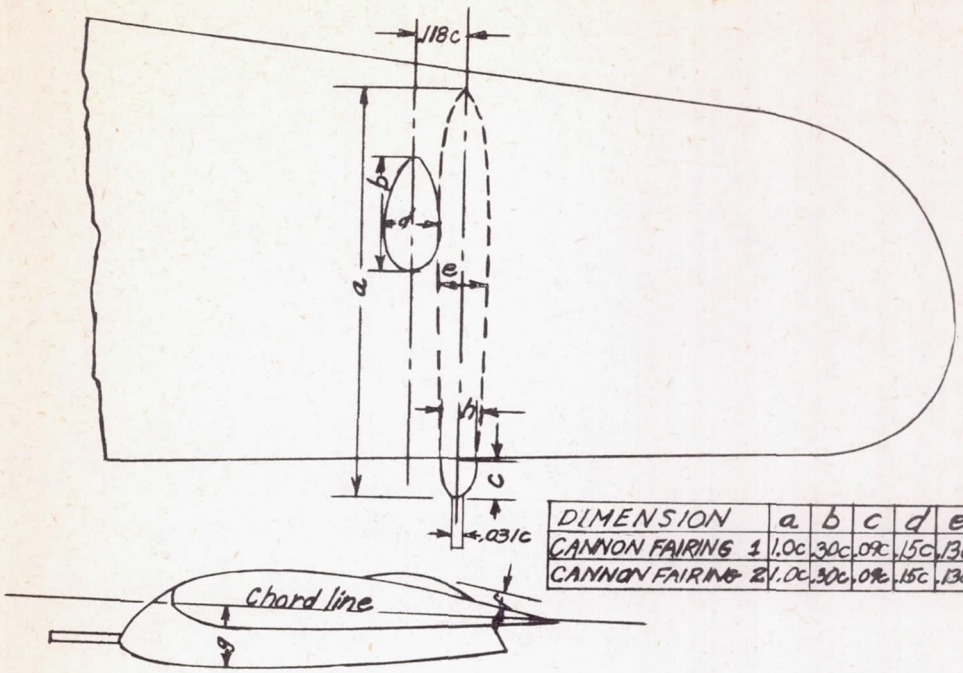

DIMENSION	a	b	c	d	e	f	g	h
CANNON FAIRING 1	1.0c	.30c	.09c	.15c	.13c	.04c	.16c	.13c
CANNON FAIRING 2	1.0c	.30c	.09c	.15c	.13c	.04c	.16c	.09c

(a) Underslung cannon installation.

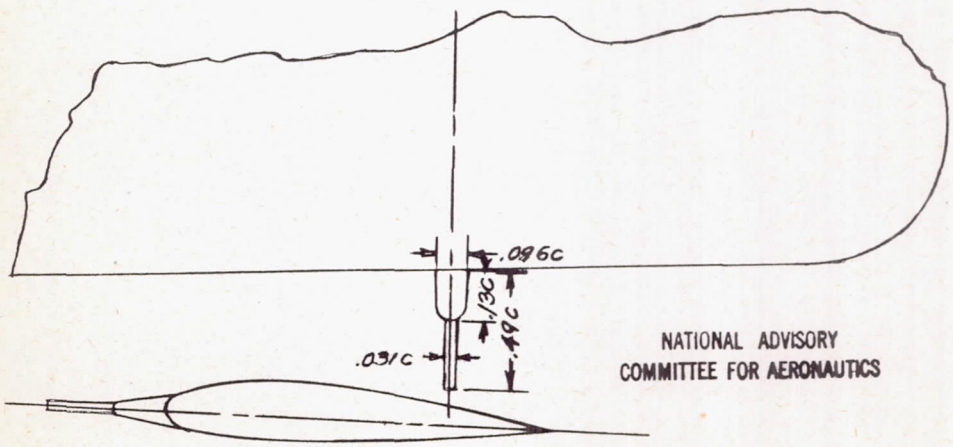

(b) Submerged cannon installation.

Figure 29.- Wing-cannon installation on XF2A-2 airplane.

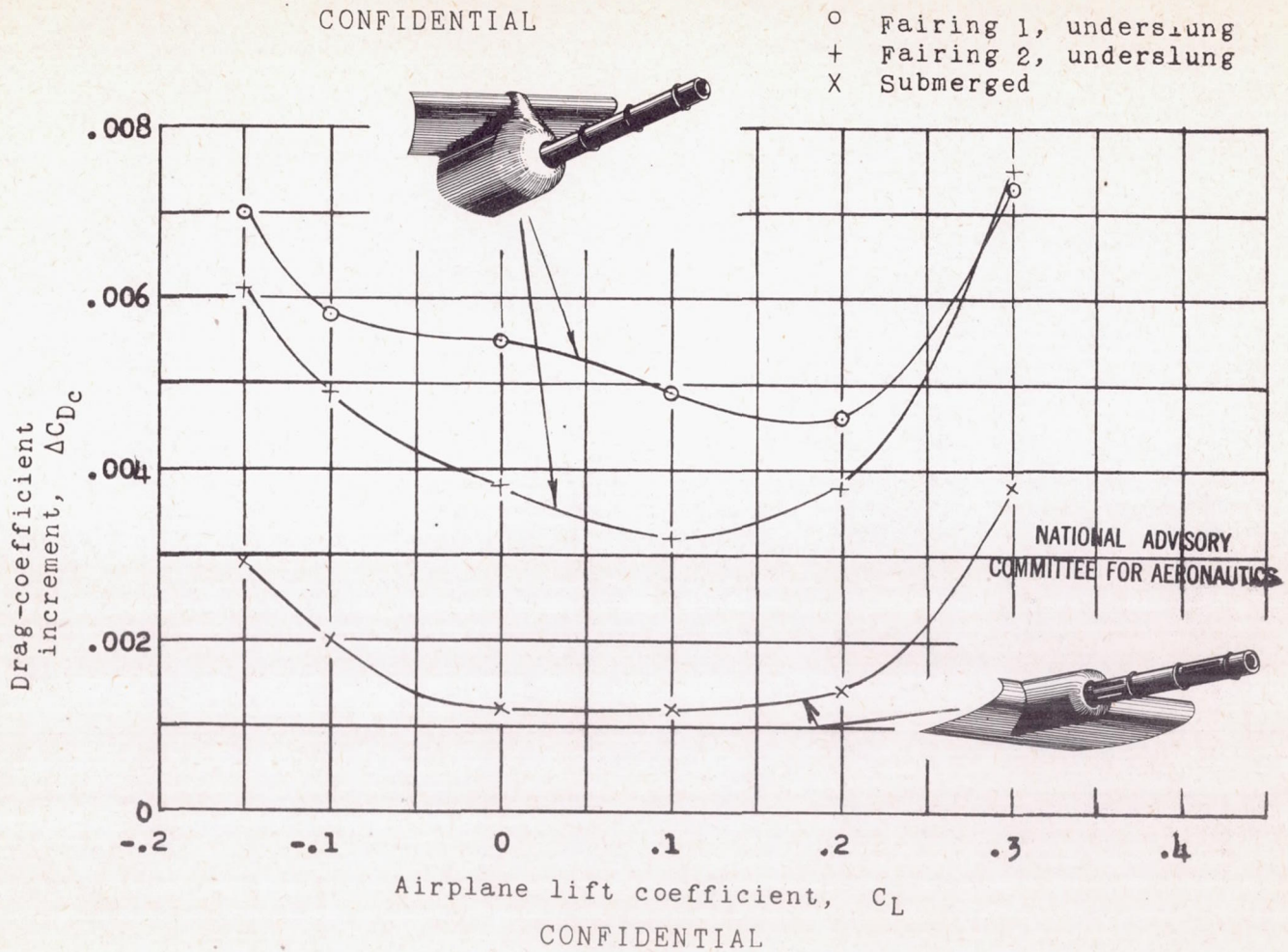

Figure 30.- Cannon drag increments on XF2A-2 airplane in Langley full-scale tunnel. $R = 5.5 \times 10^6$.

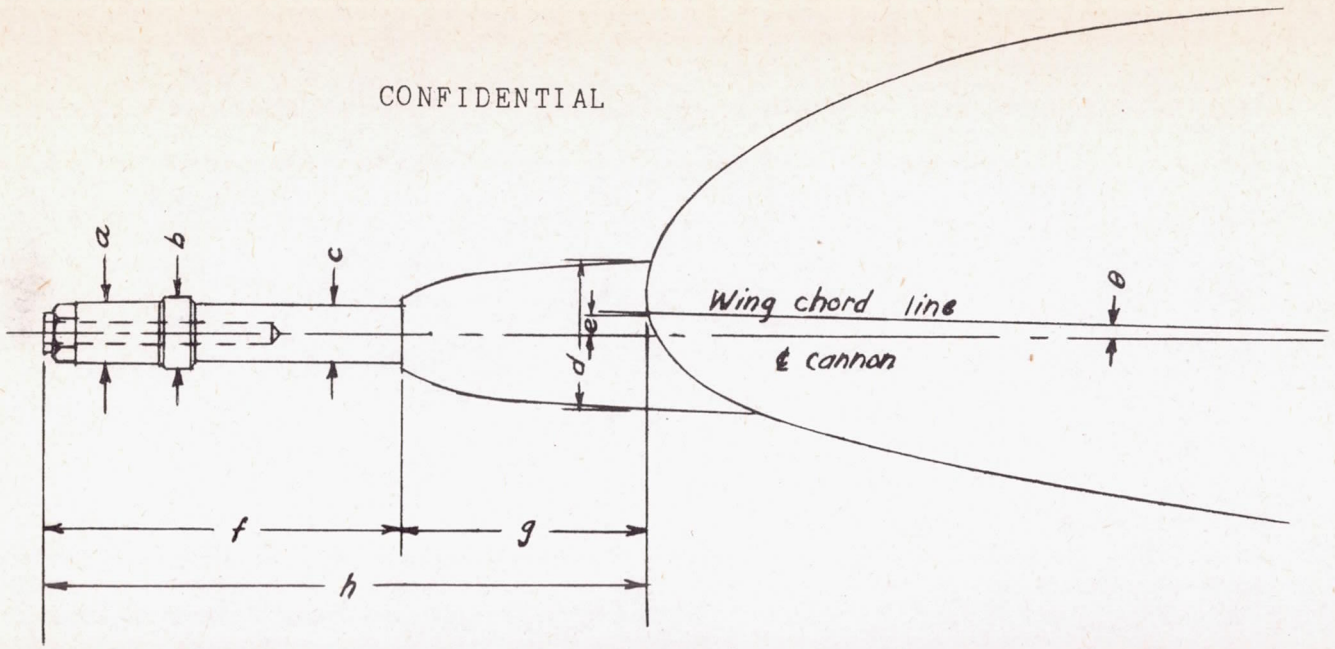

CANNON DIMENSIONS (percent c)										
NACA SECTION	CHORD	θ	a	b	c	d	e	f	g	h
23015	24	1°39'	1.595	1.888	1.458	3.970	0.629	9.880	6.665	16.545
65,3-418	24	1°28'	1.595	1.888	1.458	3.970	0.629	9.880	6.665	16.545
66(215)-216	36	1°18'	2.130	2.516	1.945	6.110	1.222	13.130	20.970	34.100
66(215)-216	36	1°4'	1.595	1.888	1.458	3.970	0.629	9.880	6.665	16.545
66(215)-216	24	1°4'	1.595	1.888	1.458	3.970	0.629	9.880	6.665	16.545

NATIONAL ADVISORY
COMMITTEE FOR AERONAUTICS

Figure 31.- Twenty-millimeter cannon installations on low-drag and conventional airfoil sections.

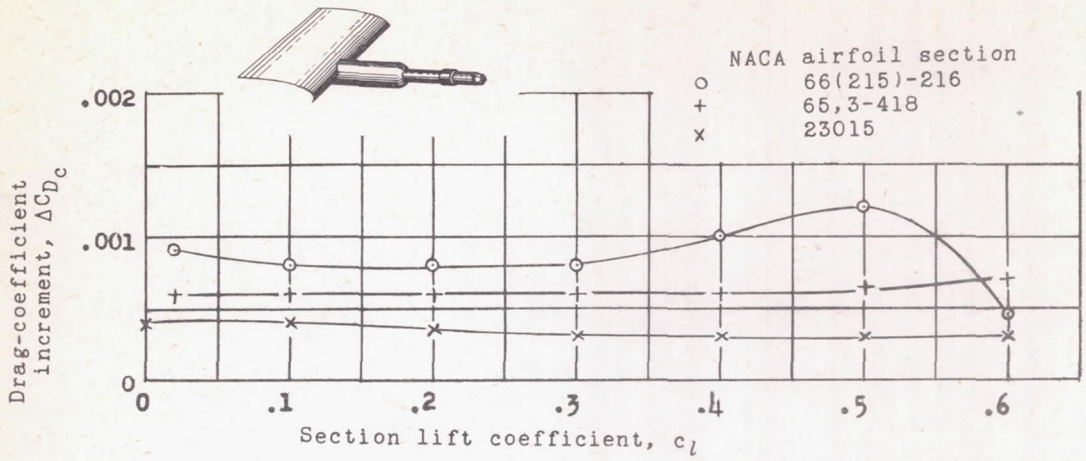

(a) Drag increments of cannon on three NACA airfoil sections.

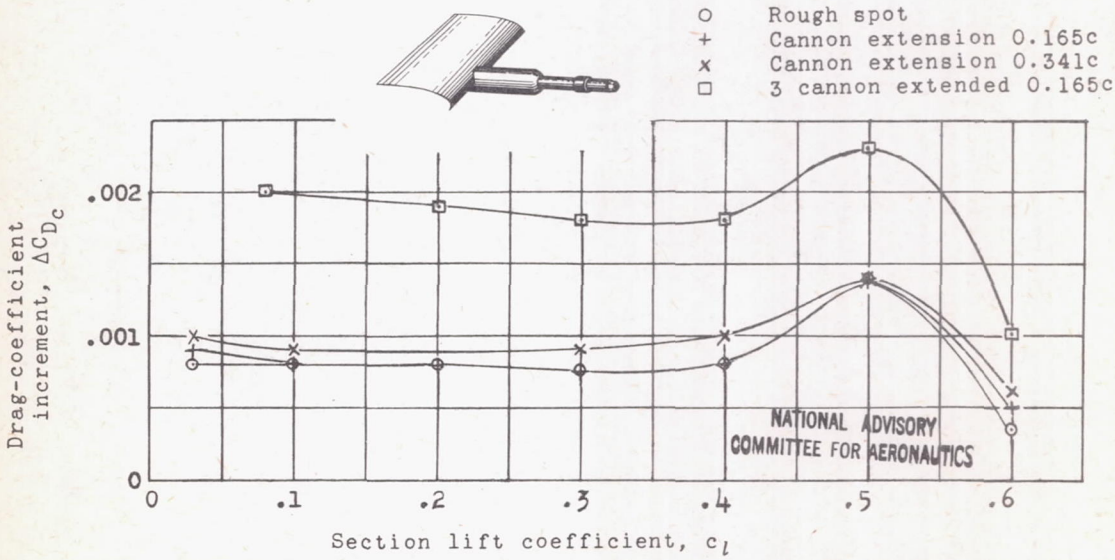

(b) Drag increment of two cannon extensions compared with drag increment of rough spot on NACA 66(215)-216 airfoil section.

Figure 32.- Twenty-millimeter cannon installations in Langley two-dimensional low-turbulence pressure tunnel. $R = 6.0 \times 10^6$.

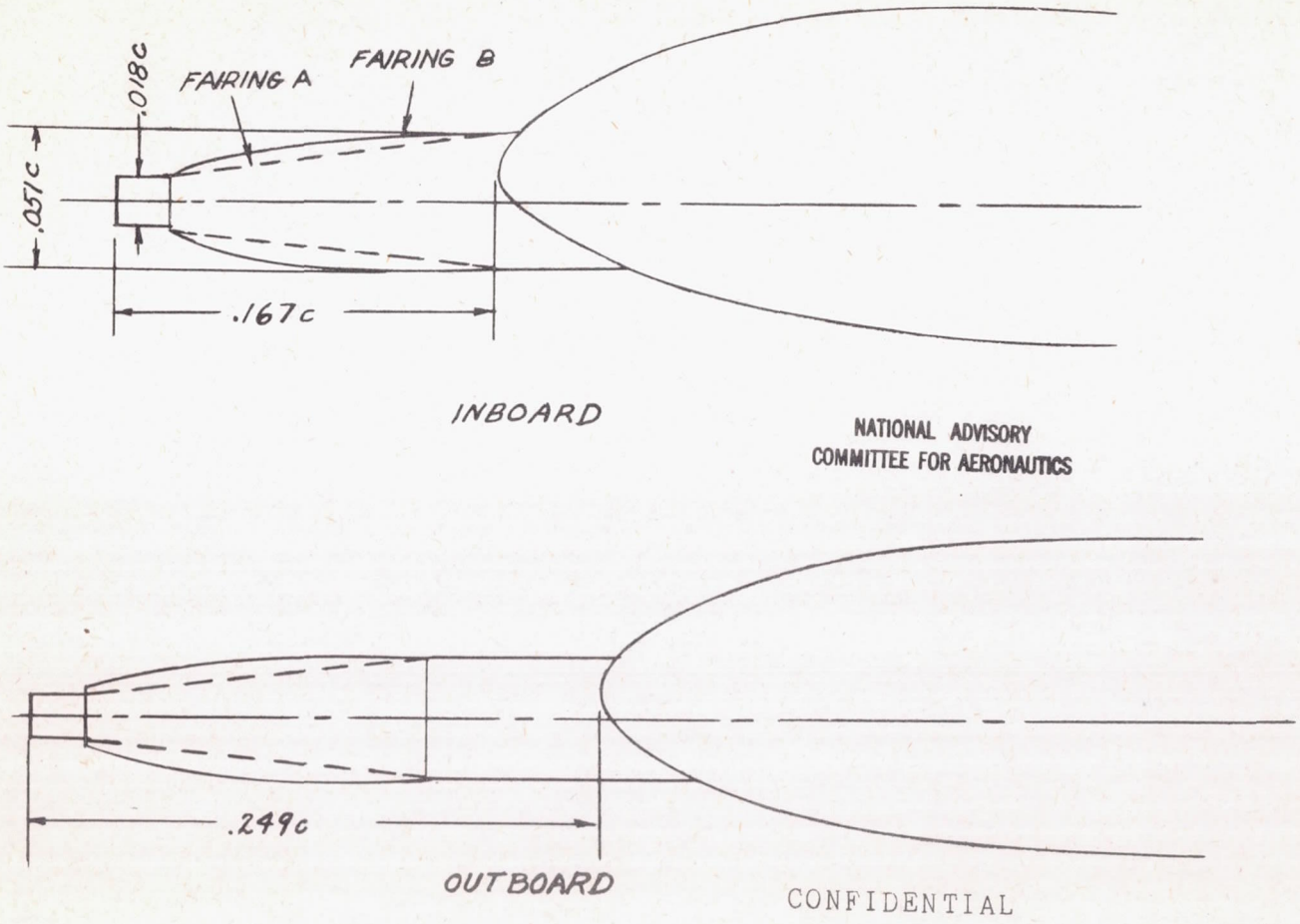

Figure 33.- Cannon installations on XF14C-2 airplane.

CONFIDENTIAL

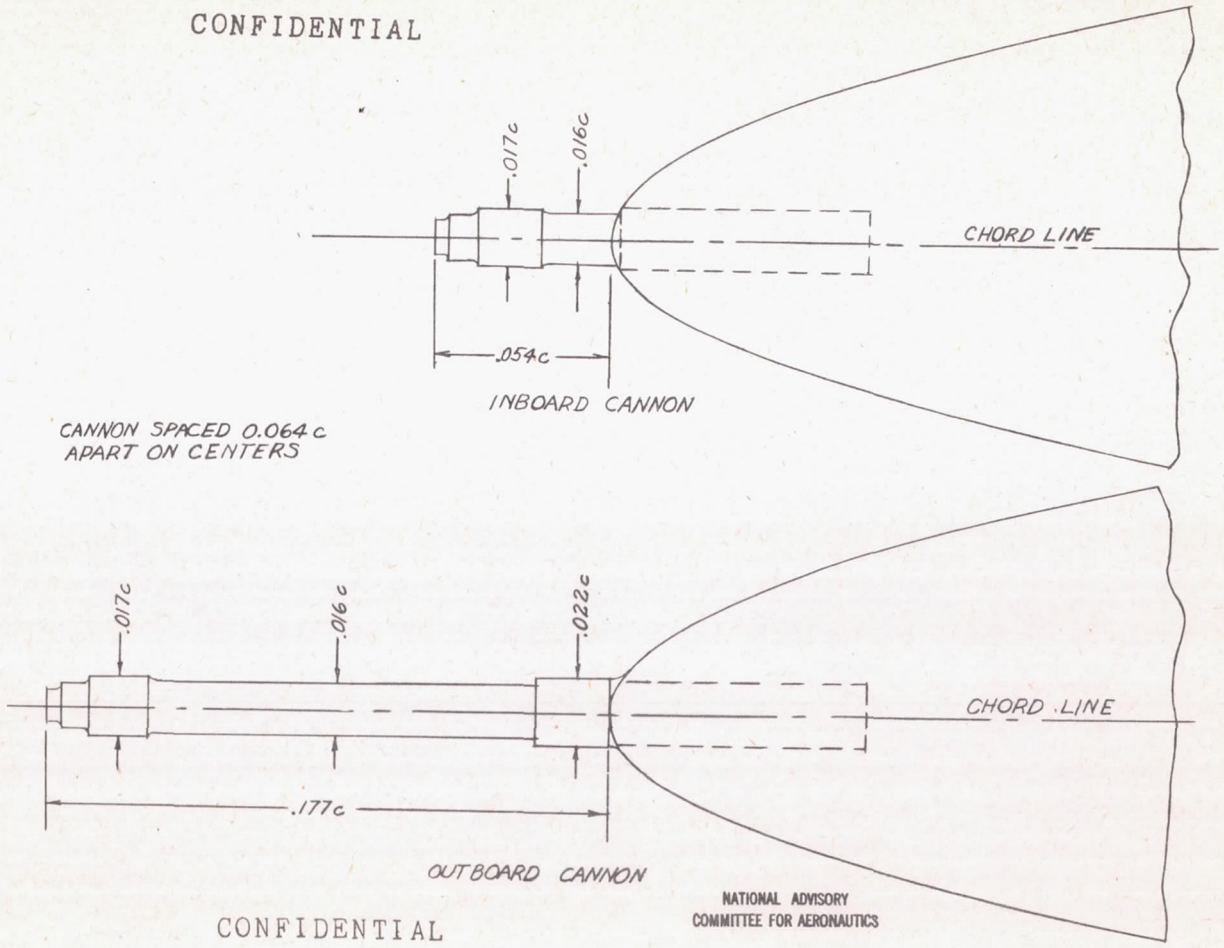

CONFIDENTIAL

Figure 34.- Cannon installations on model of XF6F airplane.

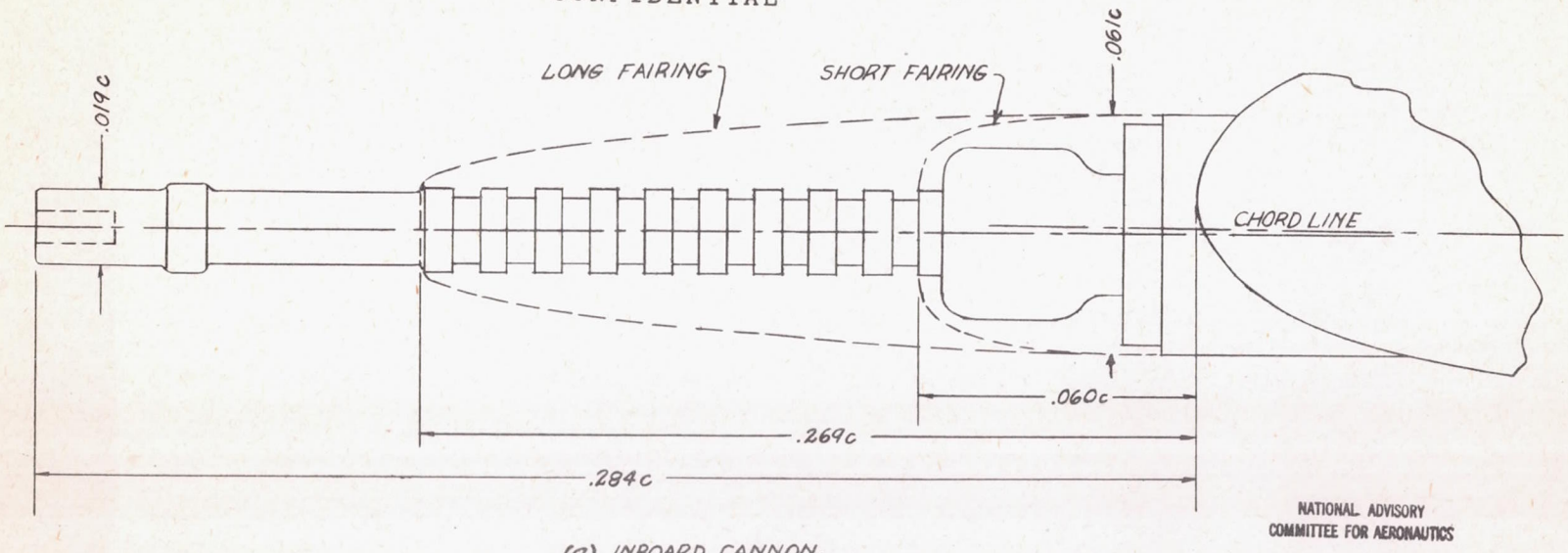

(a) INBOARD CANNON.

Figure 35.- Cannon installations on model of XF4U-1 airplane.

CONFIDENTIAL

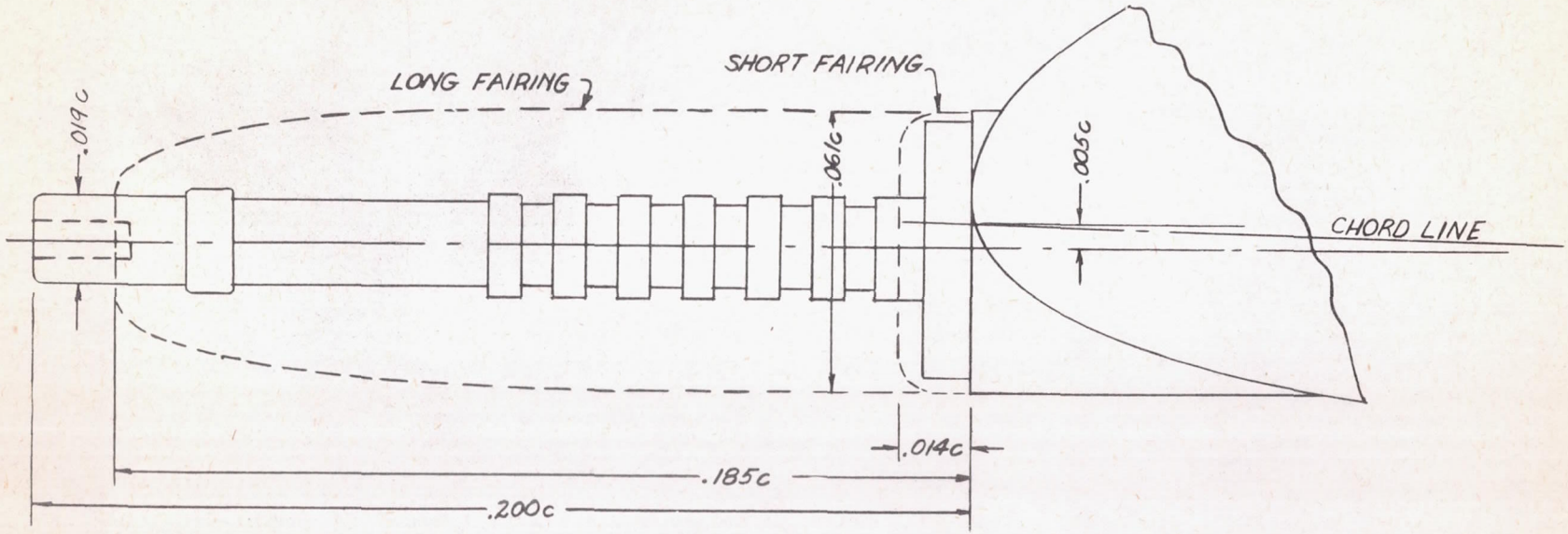

CONFIDENTIAL

(b) OUTBOARD CANNON.

NATIONAL ADVISORY
COMMITTEE FOR AERONAUTICS

Figure 35.- Concluded.

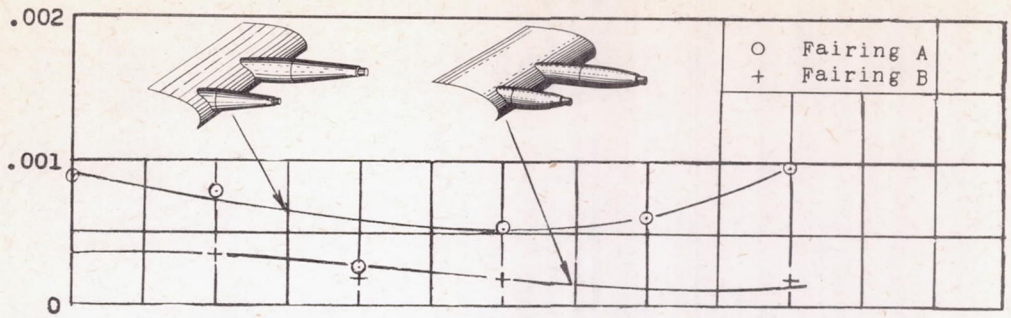

(a) Cannon installations on model of XF14C-2 airplane in Langley 19-foot pressure tunnel. $R = 5.5 \times 10^6$.

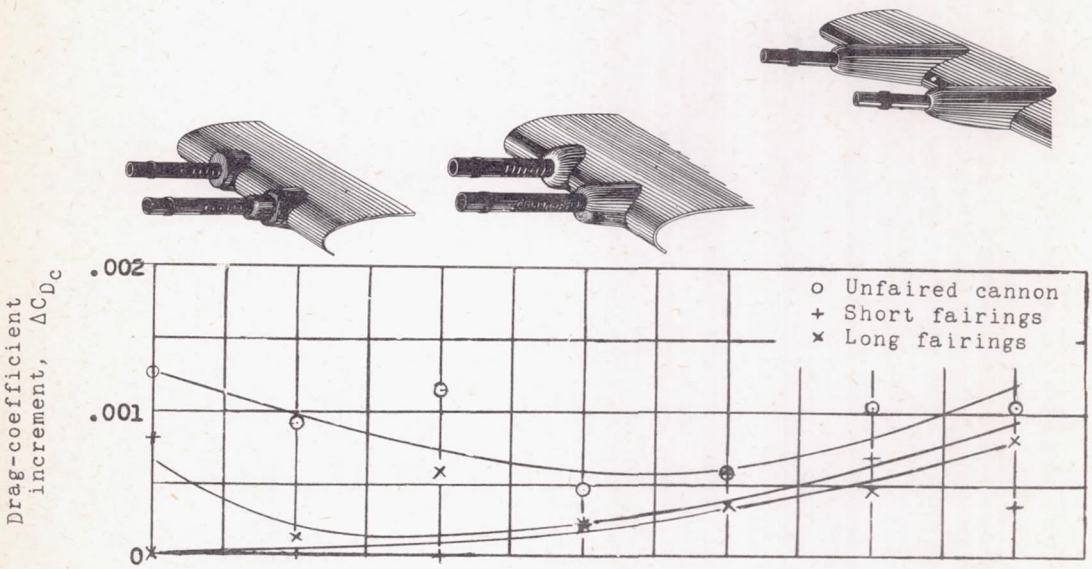

(b) Cannon on model of XF4U-1 airplane in Langley 19-foot pressure tunnel. $R = 2.75 \times 10^6$.

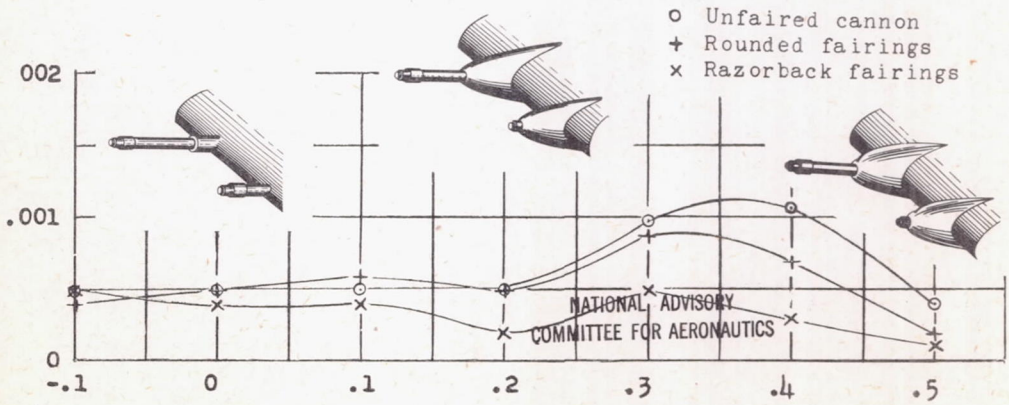

(c) Cannon installations on model of XF6F airplane in Langley 19-foot pressure tunnel. $R = 6.15 \times 10^6$.

Figure 36.- Drag increments of several 20-millimeter cannon installations.

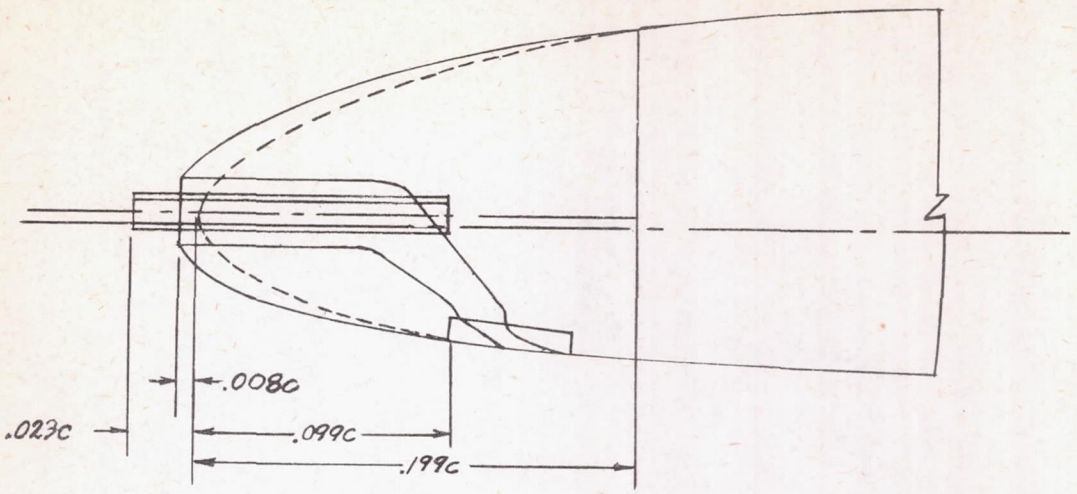

(a) Short fairings and cannon.

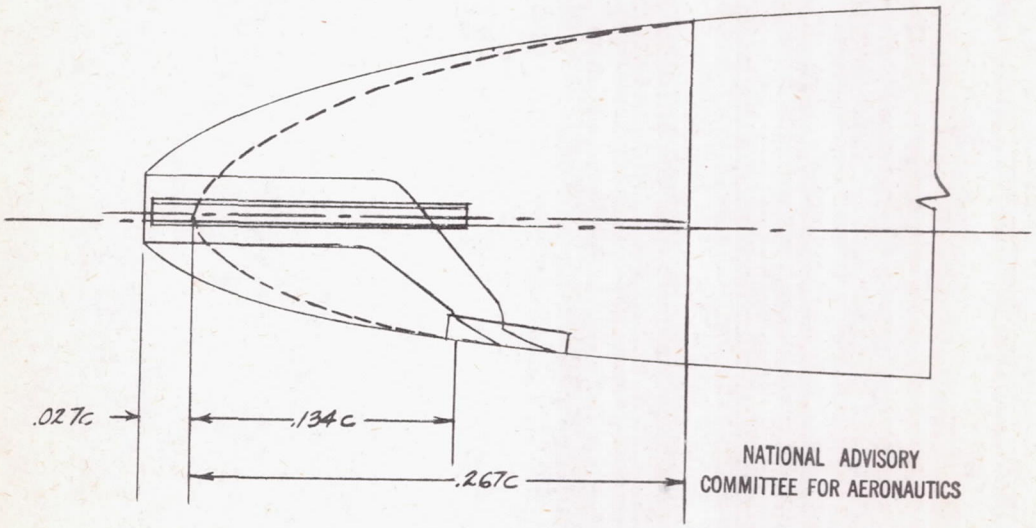

(b) Long fairings and cannon.

Figure 37.- Cannon and fairing installations on model of wing of XA-41 airplane. Cannon are centered 0.005c and 0.010c above chord line. Fairings are circular in cross section.

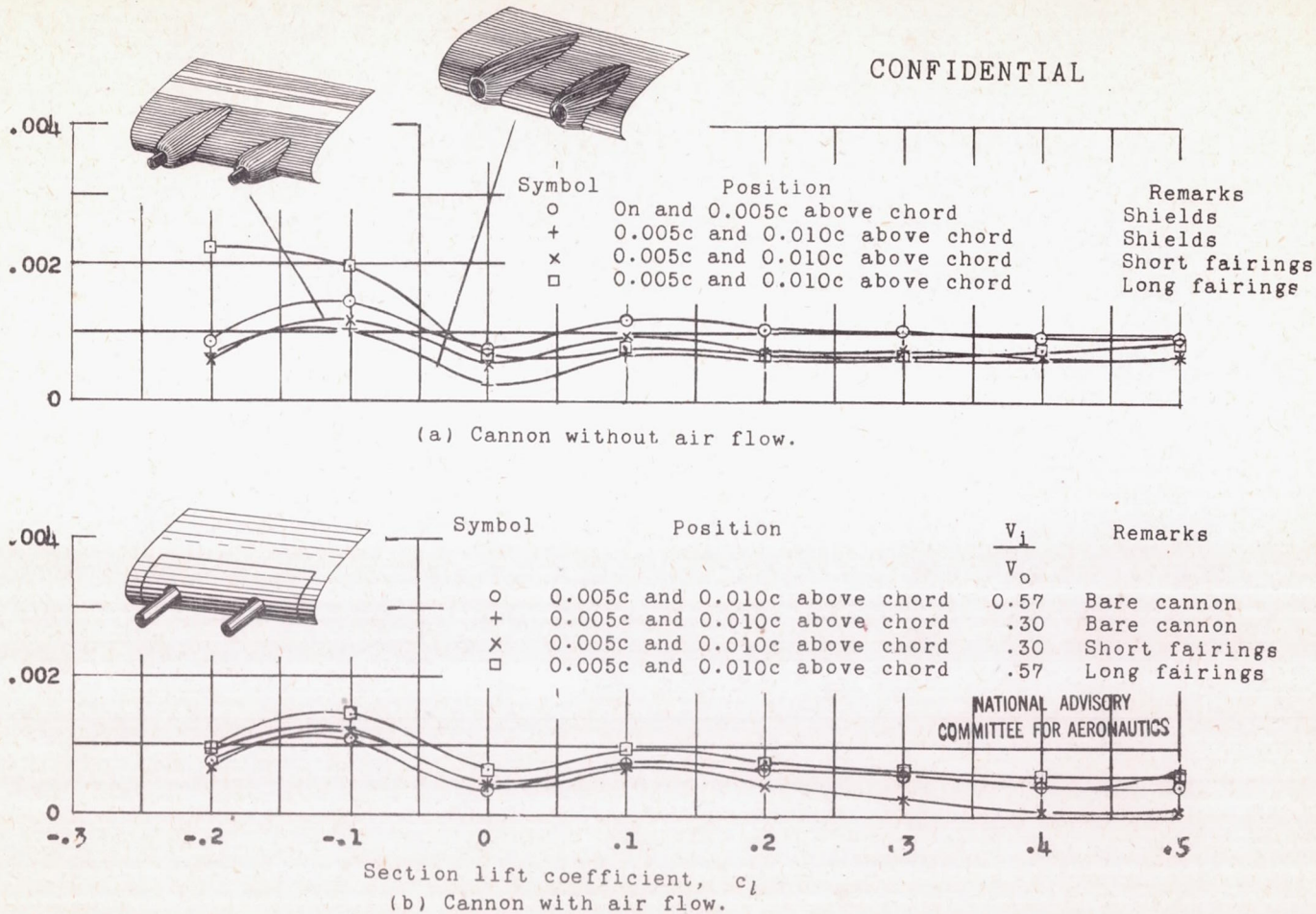

Figure 38.- Several cannon installations on model of wing of XA-41 airplane in Ames 7- by 10-foot tunnel. $R = 6.35 \times 10^6$. Holes around cannon have 0.032c and 0.034c diameters.

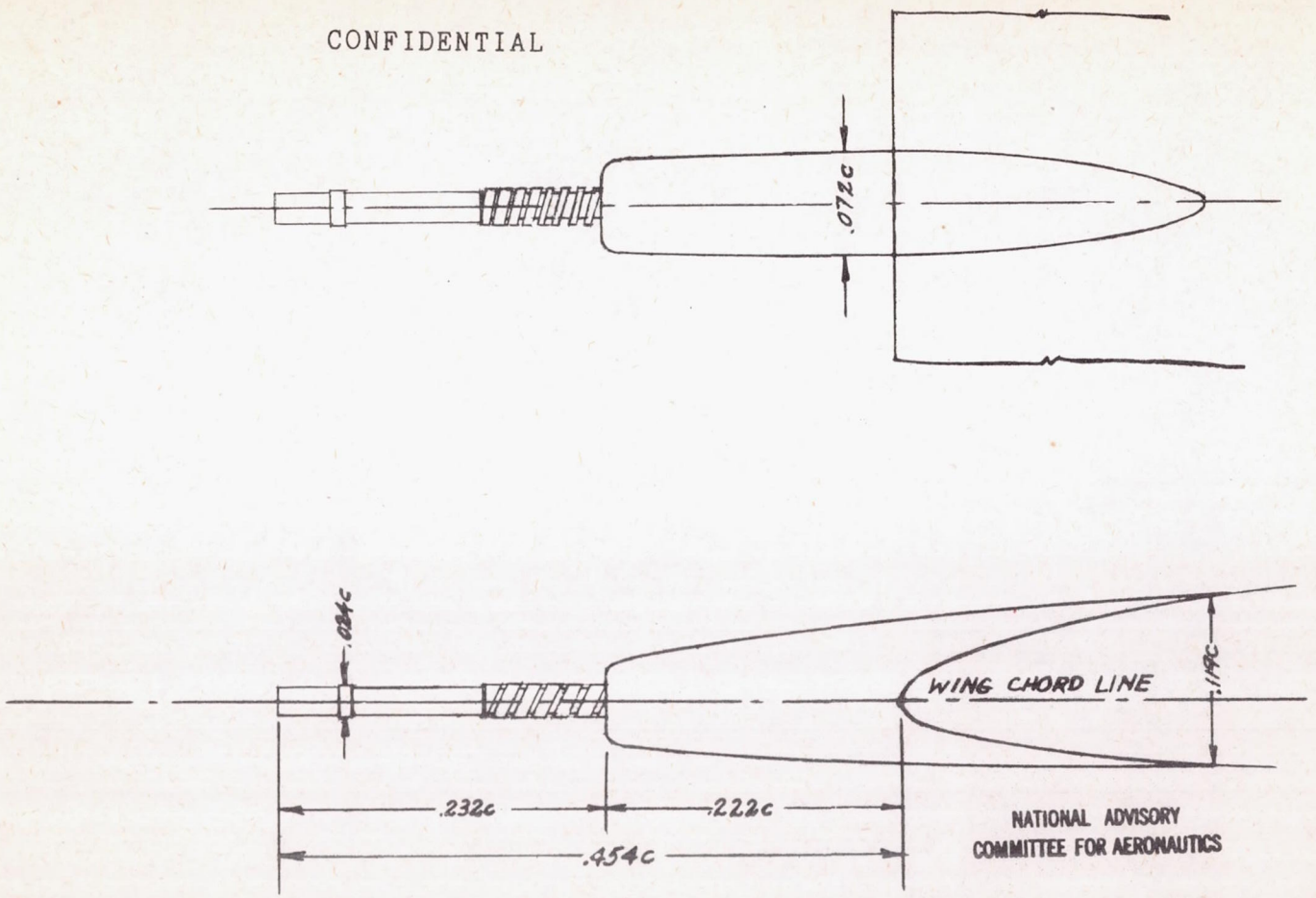

Figure 39.- Cannon installation on P-51B airplane.

CONFIDENTIAL

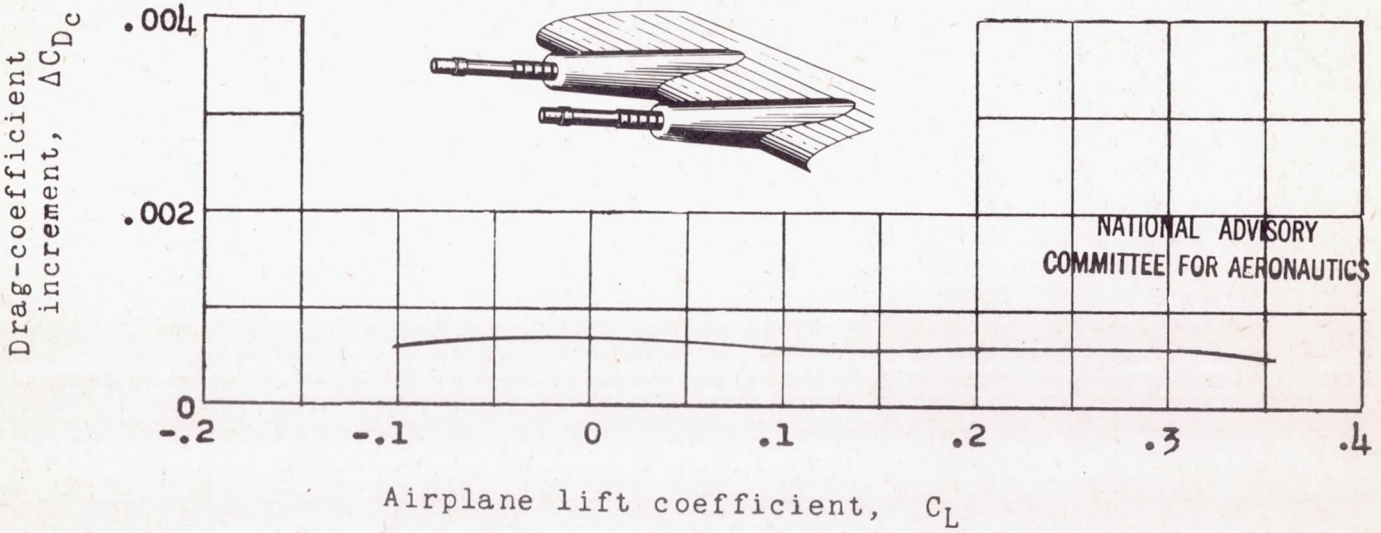

Figure 40.- Drag increments of cannon on P-51B airplane in Langley full-scale tunnel. $R = 6.0 \times 10^6$.

CONFIDENTIAL

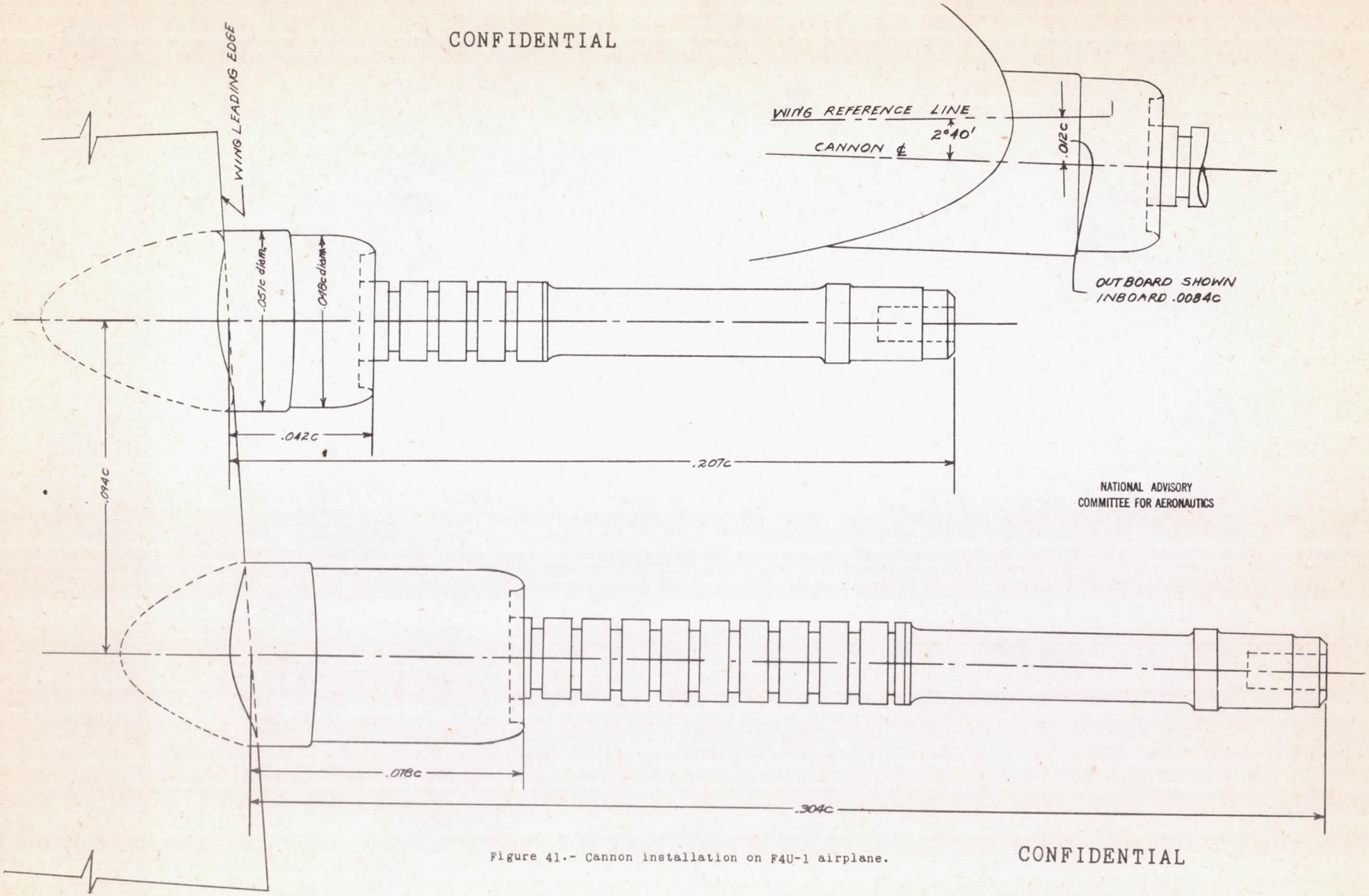

Figure 41.- Cannon installation on F4U-1 airplane.

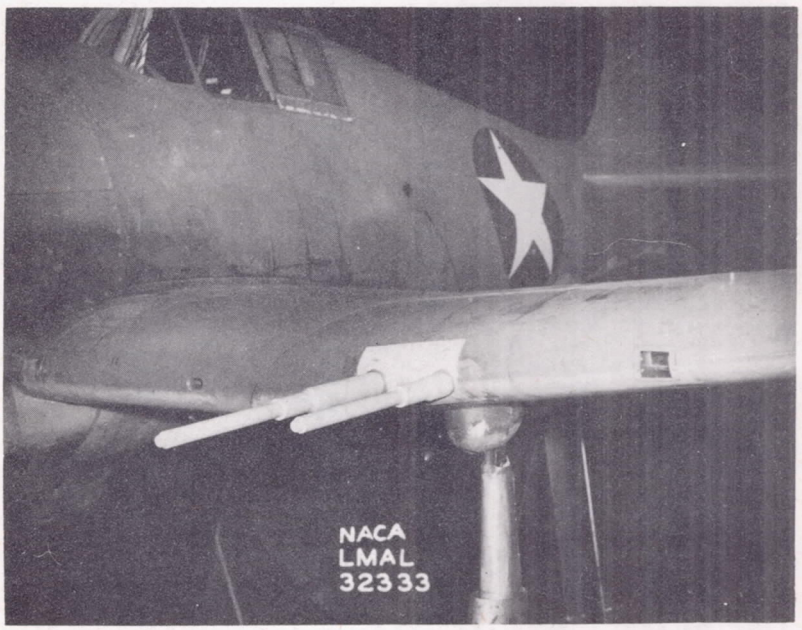

Figure 42.- Twenty-millimeter cannon mock-up on F6F-3 airplane.

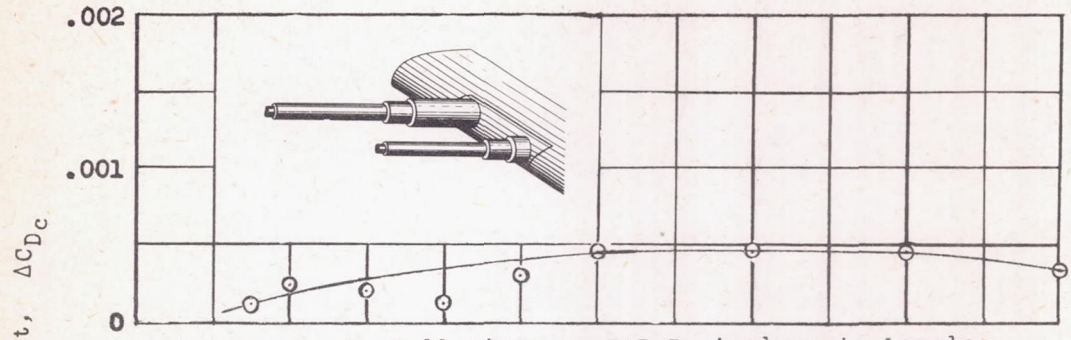

(a) Cannon installations on F6F-3 airplane in Langley full-scale tunnel. $R = 8.0 \times 10^6$ (approx.).

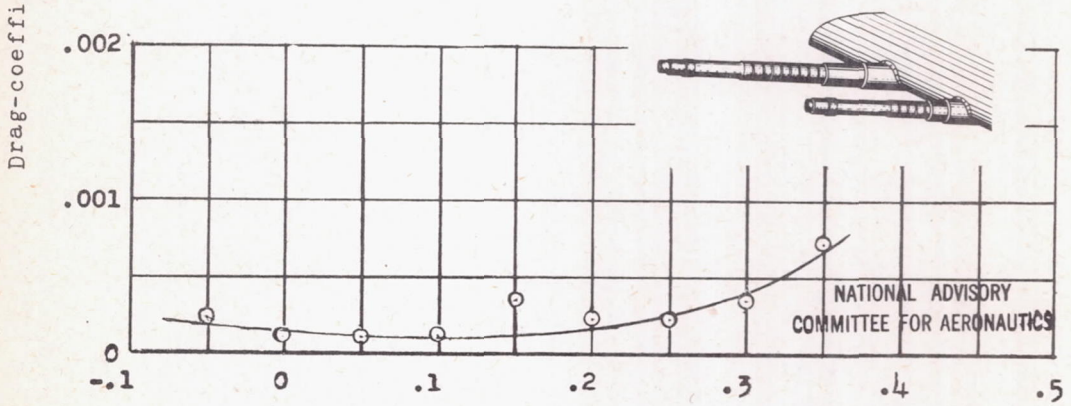

(b) Cannon on F4U-1 airplane in Langley full-scale tunnel. $R = 7.6 \times 10^6$.

Figure 43.- Drag increments of several 20-millimeter cannon installations.